2009

Topics in quantum optical metrology

Aravind Chiruvelli
Louisiana State University and Agricultural and Mechanical College, chiruvelli@phys.lsu.edu

TOPICS IN QUANTUM OPTICAL METROLOGY

A Dissertation

Submitted to the Graduate Faculty of the
Louisiana State University and
Agricultural and Mechanical College
in partial fulfillment of the
requirements for the degree of
Doctor of Philosophy

in

The Department of Physics and Astronomy

by
Aravind Chiruvelli
B.Sc., Osmania University, Hyderabad, 2000
M.Sc., University of Hyderabad, 2002
M.S., University of Massachusetts, 2006
December, 2009

Acknowledgments

Primarily I would like to thank my advisor Prof. Hwang Lee for his wonderful guidance and support. His encouragement at my own times of doubts and his unlimited patience in correcting the drafts of the papers are invaluable. I learnt a lot of the material covered in this dissertation from his insightful thoughts.

I would like to thank Prof. Jonathan Dowling for providing me an opportunity to work in his group right from the first semester of my graduate study. Although he had extremely busy schedule, he always had time to answer any question I might have. I also thank you for sending me to the conferences.

I would like to thank Dr. Kurt Jacobs for allowing me to work with him in my first project as a graduate student. I sincerely thank his generosity for making me the lead author of the paper. I also thank you for the patience you have shown in the duration of the project.

I would like to thank Dr. Thomas Kutter for being on my committee. I would also like to thank Prof. Milen Yakimov of Department of Mathematics for being on my committee as deans representative.

I would like to thank Prof. Seth Lloyd of MIT for giving me an opportunity to work with him. I thank Dr. Prasanta. K. Panigrahi at IISER, Kolkata for encouraging me to work remotely on a project while I was a Masters student at UMass, Boston and also for his support during my study at University of Hyderabad.

There are number of people in my family with out whose support I simply will not be able to pursue doctoral studies. First, My parents. I cannot thank enough my mother Kamala and father Ramamurthy for their numerous sacrifices all the way and their support and freedom in allowing me to choose a path of my own, is indispensable. Thank you mom and dad. I also would like thank my wife Madhavi for bearing with me and being always

there for me. I thank my sisters Aruna and Anitha who helped me taking care of the family while I was away from home. I also would like to thank grand parents, who has a significant role in my upbringing. Particularly my grandfather late. P. Narasimhaih. To all these people I dedicate this thesis.

I would like to thank my very dearest uncles Ramana and Murali and my friends Sri Ram, Shravan, Indira, Prasad, Gopi, Raju for their help and encouragement in my achievements.

Table of Contents

Abstract

Quantum optical metrology deals with estimation of an unknown parameter by exploiting the non-classical properties of the light. The unknown parameter that we are trying to estimate is the optical phase. Precise optical phase measurement has been a well-known problem and has many applications, most notably the gravitational wave detection.

In this thesis we investigate the interferometric measurement schemes. We consider the parity detection for a class of input states that have been shown to exhibit sub-shot noise limited phase estimate with their respective detection schemes. Our results indicate that the parity detection applies to all these strategies with various input states and thus acts as a unified detection scheme towards the goal of interferometric phase estimates beyond the shot-noise limit.

We also consider the performance of the so-called optimal state with the canonical phase measurement scheme that was proposed by Sanders and Milburn [Phys. Rev. Lett.**75**, 2944 (1995)] in presence of photon loss. The model for photon loss is a generic fictitious beam splitter and the analytical treatment requires density matrix approach rather than the state-vector formalism. We present full density-matrix calculations. Our results indicate that, for a given amount of loss, the phase estimate saturates but does not diverge as one would expect with increasing the loss.

Finally, we study the continuous measurement and feedback schme with optical homodyne detection for a single optical qubit. We found a protocol that speeds up the rate of increase of the average purity of the system and generates a deterministic evolution for the purity in the limit of strong feedback

1 Introduction

"Traveler, there are no paths. Paths are made by walking".

-Antonio Machado.

At the turn of the century, in 1900, Max Planck laid a path by making a bold assumption of discrete energy during his attempt to explain the spectrum of radiation emitted by a blackbody. The problem Planck was trying to address was, why the intensity of radiation emitted at certain wavelength depends solely on the temperature of the body and is independent of the material with which it is made. The crux of the Planck's success is the assumption that the oscillators in the walls of blackbody can only absorb or emit radiation in discrete units proportional to the frequency of the emitted radiation.

Although Planck himself was not entirely convinced of this discovery, Albert Einstein in 1905 successfully applied the Planck's idea of discrete energy to the phenomenon called photo-electric effect, where light shined on a metal knocks out electrons and the emitted electrons have energy proportional to the frequency of the incident light and independent of the intensity of the incident light. The works of Planck and Einstein have led to the quantum description of nature-quantum mechanics.

Despite these early works were in the direction of quantized form of light –an electromagnetic field–a complete quantum treatment of emission and absorption of light came only when P. A. Dirac in 1927 quantized the electromagnetic field and a quantum description of optics–quantum optics–was available [1] and the concept of *photon* was beginning to gain its importance. A breakthrough in quantum optics came in 1963 with the quantum formulation of optical coherence by R. J. Glauber [2] which led to photon counting and photon statistics and thereby fully established the field of *quantum optics*. The invention

of Microwave Amplification by Stimulated Radiation(MASER) and Light Amplification by Stimulated Amplification of Radiation(LASER) based on the quantum description of emission and absorption allowed experiments on various concepts associated with the theory of quantum optics.

As with any science, all theoretical models must be backed by experiments where measurements on certain physical parameters are carried out. In quantum mechanics the description of a state of a physical system is radically different from the classical counterpart. A quantum state (to be described later) or a wave function has an inherent probability, due to which a measurement on a quantum state often yields inconclusive results. Therefore, it makes more sense to talk about the estimates rather than a definite results.

Can quantum mechanical properties of a state be used for improving sensitivity and resolution in estimating a physical parameter? This is precisely the question *Quantum metrology* deals with. Quantum optical metrology is an attempt to answer the above question using light quanta–photons, and the quantum mechanical properties of the state in this context are the existence of non-classical correlations between the photons in various modes. The physical parameter that is of primary concern in the context of quantum optical metrology is the optical *phase*.

Precise measurement of an optical phase is of extreme value in the detecting gravitational waves [3] and has applications towards building quantum sensors [4]. In order to *measure* the phase quantum mechanically, one needs an observable that can be described by an hermitian operator. A properly defined phase operator is still a subject of debate [5]. This calls for an estimation of phase rather than directly measuring the phase.

In the next two sections I shall briefly review quantum mechanics and quantum optics with the topics that are pertinent to the work in this thesis.

1.1 Brief Review of Quantum Mechanics

The cornerstone of quantum information and computation is the superposition principle of quantum mechanics [6]. Superposition principle states that if $|\psi\rangle$ and $|\phi\rangle$ are two allowed states of a physical system, then any linear combination $\alpha|\psi\rangle + \beta|\phi\rangle$ is also an allowed physical state, with the normalization condition $|\alpha|^2 + |\beta|^2 = 1$. As a consequence of linearity of quantum dynamics, the superposition principle concludes that the system not necessarily be either in state $|\psi\rangle$ or in state $|\phi\rangle$ at a given time, but *can be in both states at the same time*. This is an hallmark of quantum mechanics with no classical analogue. We begin this review with a discussion of quantum states and shall review only the topics that are pertinent to the work in this thesis.

1.1.1 Pure States and Mixed States

A d dimensional quantum system can be described by a set of orthonormal basis $\{|i\rangle\}$ where $i = 1, 2, \ldots .d$. Here orthonormal indicates $\langle i|\ j\rangle = \delta_{i,j}$. The space described by these orthonormal basis is called as Hilbert space. A quantum state

$$|\psi\rangle = \sum_{i=1}^{d} \psi_i |i\rangle \tag{1.1}$$

is a pure state when $|\psi\rangle$ can be expressed as a coherent superposition of the basis states and not as a statistical ensemble of the basis states. A mixed state is a statistical ensemble denoted by ρ and is also called as density operator or density matrix.

Formally the density operator of a pure state $|\psi\rangle$ is given as:

$$\rho \equiv |\psi\rangle \langle\psi| \tag{1.2}$$

and satisfies the following properties:

1. ρ is positive and Hermitian, $\rho^\dagger = \rho$
2. Tr[ρ]=1. This is due to the normalization of $|\psi\rangle$

3. $\rho^2 = |\psi\rangle \langle\psi|\psi\rangle \langle\psi| = \rho$.

By virtue of (2) and (3) it immediately follows that for a pure state

$$\mathrm{Tr}[\rho^2] = 1. \tag{1.3}$$

One immediately can construct the density operator for a mixed state. To keep the discussion more generic, let $\{|i\rangle\}$ be and orthonormal basis: $\langle i|j\rangle = \delta_{i,j}$ of an N dimensional Hilbert space. We can define

$$\rho = \sum_{i,j=1}^{N} p_{ij} |i\rangle \langle j| \tag{1.4}$$

Because of the condition (2) we get $\sum_i p_{ii} = 1$ implying that $0 \leq p_{ii} \leq 1$. When the density operator is represented as a matrix, the diagonal elements corresponds to the probabilities associated with the basis states. So we obtain the relation

$$\mathrm{Tr}[\rho^2] = \sum_i p_i^2 \leq 1. \tag{1.5}$$

In Eq. 1.5 the upper bound is true for only pure states and the inequality holds for a mixed state. This means that given any state as a density matrix, we can decide directly weather it is pure or mixed by evaluating $\mathrm{Tr}[\rho^2]$.

1.1.2 Degree of Impurity

In the light of Eq. (1.4) and Eq. (1.5), we find that in an N dimensional Hilbert space, the state with equal probability of basis state would be maximally mixed. This occurs when $p_i = \frac{1}{N}$ and the quantity $\mathrm{tr}[\rho^2]$ takes the minimum value of $\frac{1}{N}$. This immediately gives the the expression for the state which is *maximally mixed* as:

$$\rho = \frac{1}{N}\mathbf{I}. \tag{1.6}$$

The *impurity* of a state, also called as linear entropy, is quantified as:

$$L \equiv 1 - \mathrm{tr}[\rho^2] \tag{1.7}$$

Since for a pure state $\mathrm{Tr}[\rho^2]$=1 and for pure state and $\mathrm{Tr}[\rho^2] = \frac{1}{N}$ for a maximally mixed state, the impurity L is bounded by:

$$0 \leq L \leq 1 - \frac{1}{N}. \tag{1.8}$$

1.1.3 Two–Level Quantum System: Qubit

A two–level quantum system has many applications. Examples of these systems are the spin-1/2 particles such as electrons, or photons with the horizontal or vertical polarizations. If the two possible states of such a system are viewed as bits 0 and 1 in classical computers, the elementary carriers of quantum information can be denoted by states $|0\rangle$ and $|1\rangle$. Those are known as *qubits*. By virtue of the superposition principle, we can have a qubit as a linear combination of both $|0\rangle$ and $|1\rangle$. For a two–level system $\{|0\rangle, |1\rangle\}$ forms the orthonormal basis of the two dimensional Hilbert space and a qubit is written as

$$|\psi\rangle = \alpha\,|0\rangle + \beta\,|1\rangle \tag{1.9}$$

with the normalization condition $|\alpha|^2 + |\beta|^2 = 1$. The orthonormal basis $\{|0\rangle, |1\rangle\}$ is also called as *computational basis*.

The coefficients α and β can take any value subject to the normalization and a generic pure state qubit is written as:

$$|\psi\rangle = \cos\frac{\theta}{2}\,|0\rangle + e^{i\phi}\sin\frac{\theta}{2}\,|1\rangle\,. \tag{1.10}$$

Geometrically a pure state qubit can be represented as a point (θ, ϕ) on a unit sphere called the Bloch sphere.

To express the qubit as a density operator we can use the Pauli spin operators

$$\sigma_x = \begin{pmatrix} 0 & 1 \\ 1 & 0 \end{pmatrix};\quad \sigma_y = \begin{pmatrix} 0 & -i \\ i & 0 \end{pmatrix};\quad \sigma_z = \begin{pmatrix} 1 & 0 \\ 0 & -1 \end{pmatrix}$$

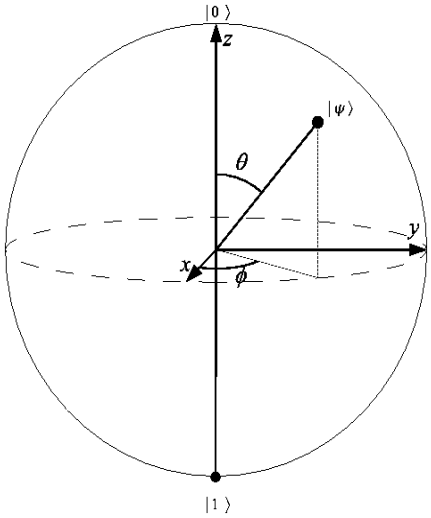

FIGURE 1.1. Bloch vector in a Bloch sphere and its parametrization by θ and ϕ.

which satisfy the commutation relation $\sigma_i\sigma_j - \sigma_j\sigma_i = i\epsilon_{ijk}\sigma_k$, and $\sigma_i^2 = 1$. Thus the qubit as density matrix in terms of the Pauli operator basis is:

$$\rho = \frac{1}{2}(\mathbf{I} + \vec{\mathbf{r}} \cdot \vec{\sigma}), \tag{1.11}$$

where r is called as the Bloch vector, whose components are given as $r_i = \mathrm{tr}[\rho\sigma_i] = \langle\sigma_i\rangle$. This immediately leads to

$$\mathrm{Tr}[\rho^2] = \frac{1}{2}(1 + |r|^2) \tag{1.12}$$

But for a 2–dimensional quantum system, from Eq. (1.8), we have $0.5 \leq \mathrm{Tr}[\rho^2] \leq 1$. Therefore the magnitude of the Bloch vector has an upper bound: $|r|^2 \leq 1$, where the upper limit is for the case of a pure state. The impurity can now be written as

$$L = 1 - \mathrm{tr}[\rho^2] = \frac{1}{2}(1 - |r|^2) \tag{1.13}$$

This means that for a mixed state the Bloch vector lies within the Bloch sphere. For a maximally mixed state $L = 0.5$ and $r = 0$.

Qubits are particularly important in the field of quantum information and quantum computing. In 1982 Richard. P. Feynman discussed the idea of simulating quantum physics with classical computers and showed that a quantum system can be efficiently simulated

only with another quantum system, leading to the idea of building a computer based on the laws of quantum mechanics [7]. Later in 1986 he discussed the idea of quantum mechanical computers [8]. The real breakthrough came in 1994 when Peter. W. Shor discovered the factorization algorithm based on quantum mechanics, in which he proved that one can achieve an exponential speed-up in factoring large integers, over the most efficient classical algorithm [9]. This discovery gave an enormous momentum and turned the field of quantum information and computation [10] from an academic quest to a technological challenge.

Before we conclude the discussion on qubit it is worth mentioning that any two–level quantum mechanical system can be used as qubits and the availability of superpositions makes it even richer. It can be observed that in classical computers the bit 0(1) could be voltage on(off) and are resistant to any physical forces. In quantum computers the qubits are physical states and could be manipulated by applying suitable force fields. Therefore we can construct the logic gates for a qubit with suitably varying electric or magnetic fields [11].

1.1.4 Quantum Measurements

Since the formulation of quantum mechanics, measurements on a quantum state has been a debatable topic. This is mainly due to the intuition developed by the classical physics, that a measurement on a physical system must yield definite and conclusive result. Due to the existence of superposition often in quantum mechanics, we can only predict probabilities of outcomes. A quantum state will be changed probabilistically when a measurement is done.

Another intuition along the line of classical physics is that the act of measurement does not alter the state of the system. This is not the case in quantum system and an act of measurement invariably disturbs the system and leaves the system in the eigenstate of the measurement observable which is the famous wave function collapse. This discrepancy

between what is believed along the classical line of thought and the quantum description gave the problem of quantum measurement a metaphysical picture.

- **Projective Measurements and POVM**

This formalism was first developed by John Von Neumann and is also called as strong measurements. In quantum mechanics the observable are represented by a Hermitian operators $\hat{O} = \hat{O}^\dagger$. The eigenvalue n specifies the state which is the eigenstate $|\phi_n\rangle$ of the observable: $\hat{O}\,|\phi_n\rangle = n\,|\phi_n\rangle$. If the state before the measurement is $|\psi\rangle$, then the probability of obtaining the value n is $|\langle\phi_n|\psi\rangle|^2$.

This kind of measurements are called as projective measurements and are described by the projectors as,

$$\hat{P}_n = |\phi_n\rangle\,\langle\phi_n|\,, \tag{1.14}$$

with properties $\hat{P}_n\hat{P}_m = \delta_{nm}P_n$ and $\sum_n \hat{P}_n = 1$. The probability p_n of obtaining value n is then $\langle\psi|\hat{P}_n|\psi\rangle$. The final state $|\phi_n\rangle$ of the system after the measurement is

$$|\phi_n\rangle = \frac{\hat{P}_n\,|\psi\rangle}{\sqrt{\langle\psi|\hat{P}_n|\psi\rangle}} = \frac{\hat{P}_n\,|\psi\rangle}{\sqrt{p_n}}. \tag{1.15}$$

For a initial mixed state ρ_i the probability of obtaining the outcome n is $p_n = \mathrm{tr}[\hat{P}_n\rho_i]$. The state after the measurement, ρ_f is given as $\hat{P}_n\rho_i\hat{P}_n/p_n$. This formalism also implies that we are measuring in the basis $\{|\phi_n\rangle\}$ for $n = 1, 2, \cdots$. Also any further measurements yield the outcome n and the state does not change.

Positive Operator Valued Measure–POVM–is a generalization of the projective measurement. A set of positive operators $\left\{\hat{E}_n\right\}$ which are not necessarily the projectors, forms a POVM, when $\sum_n \hat{E}_n = 1$, while the probability of obtaining the result n is $p_n = \mathrm{tr}[\hat{E}_n\rho]$. Further, we should be able to the find operators $\hat{A}_{nk}$ such that

$$\hat{E}_n = \sum_k \hat{A}^\dagger_{nk}\hat{A_{nk}}. \tag{1.16}$$

An initial state, ρ_i is transformed to the post measurement state, ρ_f,

$$\rho_f = \frac{\sum_k \hat{A}_{nk}\rho\hat{A}_{nk}^\dagger}{\mathrm{tr}[\hat{E}_n\rho]}. \tag{1.17}$$

This measurement will in general not preserve the purity of the state. POVM reduces to the projective measurement if there exists only a single operator $\hat{A}_n$ such that $\hat{E}_n = \hat{A}_n^\dagger\hat{A}_n$. The main difference between the projective measurement and POVM is that, if a POVM is repeated we do not necessarily obtain the same result the second time and so the Von Neumann–type projective measurement is a special case of POVM [12].

- **Weak and Continuous Measurements**

The idea of weak measurements is to have rather small disturbance on the system due to the measurement. This has a trade off of learning very little about the system. A weak measurement can be formally defined with the POVM operators $\hat{A}_{nk}$ as,

$$\hat{A}_{nk} = \mathcal{C}\sum_k f_n(k,\kappa)\left|k\right\rangle\left\langle k\right|, \tag{1.18}$$

where the parameter κ can be related to the uncertainty in the final state and thus can be interpreted as the strength of the measurement. The normalization constant $\mathcal{C}$ is defined such that

$$\sum_n \hat{E}_n = \sum_n\sum_k \hat{A}_{nk}^\dagger\hat{A_{nk}} = 1. \tag{1.19}$$

The function $f_n(k,\kappa)$ characterizes the POVM and is chosen such that, when repeatedly acted upon a state $\left|\psi\right\rangle = \sum_i \psi_i\left|i\right\rangle$, it results in a final state which has a high probability of being in the state $\left|n\right\rangle$(the index of the operator $\hat{A}_{nk}$). A particular example [12] is using $f_n(k,\kappa) = e^{-\kappa(k-n)^2/4}$ in Eq. (1.18) and acting on a initial mixed state ($\rho_i = I/2$). That would result in a state whose distribution is peaked at value n and has an uncertainty of $1/\sqrt{\kappa}$ determining the strength of the measurement. Smaller κ imposes a very small disturbance on the system and thus describes a weak measurement but has a large uncertainty in the final state.

The mathematical framework of the measurement theory does not indicate the measurement time taken, but realistically there is always a certain time scale associated with any kind of measurement. A continuous measurement can be viewed as applying a sequence of weak measurements in intervals ΔT. To illustrate this point further, consider a two–level system $\{|0\rangle, |1\rangle\}$. This could correspond to a spin-1/2 system or the two polarizations of a photon. A POVM $\hat{A}_{0,(1)}$ can be defined as,

$$\hat{A}_{0,(1)} = \sqrt{\kappa}\,|0(1)\rangle\langle 0(1)| \pm \sqrt{1-\kappa}\,|1(0)\rangle\langle 1(0)|\,. \tag{1.20}$$

When $\kappa \ll 1$, Eq. (1.20) corresponds to the weak measurement and making such measurements in infinitesimally short time intervals Δt would correspond to the case of continuous measurement. Thus a continuous measurement can be regarded as the case when $\kappa \propto \Delta t$ [13, 14] because if the measurement is carried out for longer time we extract more information and for a shorter time we extract lesser information. Specifically, if $\Delta t = 0$ we extract no information and the system remains ineffective to the measuring device characterized by the POVM.

- **Master Equation**

A quantum state, in general, changes in two ways. First, it follows the unitary time evolution due to the Hamiltonian of the system which does preserve the purity of the state if the system is isolated from the environment, and not necessarily preserve the purity when there is an uncontrollable coupling to the the environment. Second, a quantum state changes probabilistically when a measurement is made. A measurement invariably disturbs the system and stochastically changes the initial state to one of the possible final states depending on the choice of the measurement. In practice both the stochastic and unitary evolution will happen. During the process of measurement, the system does undergo a stochastic change purely due to the measurement and then follows the unitary evolution till the next measurement occurs.

Under these conditions the state of the system $\rho(t)$ has a temporal evolution. A master equation describes such an evolution and is a differential equation $\dot{\rho}(t)$ by taking into account the two effects described above. For a system with Hamiltonian $\mathcal{H}_s$ a master equation in Lindblad form is given as [14, 15],

$$\frac{d\rho}{dt} = -\frac{i}{\hbar}[\mathcal{H}_s, \rho] + \sum_k [\hat{L}_k \rho \hat{L}_k^\dagger - \frac{1}{2}\hat{L}_k^\dagger \hat{L}_k \rho - \frac{1}{2}\rho \hat{L}_k^\dagger \hat{L}_k \tag{1.21}$$

where $\left\{\hat{L}_k\right\}$ called as Lindblad operators encode the effect of environment on the system. Eq. (1.21) can be interpreted as repeated applications of the POVM [12, 14, 15]. The operators $\hat{L}_k$ can be viewed as the measurements that are being done by the environment over which we have little control. Also, if we are dealing with a situation where we make measurements on a system that is perfectly shielded from environment, the operators $\hat{L}_k$ would correspond to the measurement operators.

When we make a measurement, we extract information regarding the system. A strong measurement gives more information and a weak measurement gives less. Because of the intrinsic probabilistic nature, our knowledge about the quantum system, a measurement record, effects the subsequent evolution of the system and the state would then be a conditioned state. On the other hand, if we make a measurement and ignore the result, the subsequent evolution does not have any effect due to the measurement. This is the characteristic of the conditional probability where the act of observation changes the future predictions. Classically, for a continuous measurement of a certain quantity $X(t)$, the output measurement record $r(t)$ is written as,

$$dr = X(t)dt + cdW \tag{1.22}$$

where dW is an increment of a gaussian random variable called as Wiener process [12], and would refer to the noise associated with the experiment and satisfies $dW = \sqrt{dt}$ has a zero mean, $\langle dW \rangle = 0$. The measurement record $r(t)$ can also be written using the

expectation value of $X(t)$ as,

$$dr = \langle X(t)\rangle dt + cdW', \tag{1.23}$$

where dW' is another random variable, which is uncorrelated with the dW and c is some constant. In the process of continuous measurement, one would be interested in the probability of an outcome and its evolution. That is to say, an equation that describes the evolution of the observers knowledge about $X(t)$ which would be given by the probability density $P(X,t)$ and is given as [12],

$$dP(X,t) = \frac{1}{c}(X - \langle X\rangle)PdW. \tag{1.24}$$

In the theory of quantum measurement, the quantity X would be an measurement observable and the state would correspond to the density matrix whose diagonal terms would give the probability. Thus in this case the measurement record for some detector efficiency η is written as,

$$dr = \eta \mathrm{Tr}[(X + X^\dagger)\rho]dt + \frac{dW}{\sqrt{8k}} \tag{1.25}$$

where $k = 1/(8c^2)$ and the master equation Eq.(1.21) will be,

$$d\rho = -\frac{i}{\hbar}[\mathcal{H},\rho]dt + \frac{1}{2}(2X\rho X^\dagger - X^\dagger X\rho - \rho X^\dagger X) + \sqrt{2k}(X\rho + \rho X - 2\langle X\rangle\rho)dW. \tag{1.26}$$

This equation is a special case of the Lindblad master equation, Eq.(1.21). This is to say that we only have one Lindblad operator, $\hat{X}$. If one makes the assumption $\hat{X}$ is hermitian: $\hat{X}^\dagger = \hat{X}$ and ignoring the measurement outcome, Eq.(1.26) will be simplified to

$$d\rho = -\frac{i}{\hbar}[\mathcal{H},\rho]dt - k[X,[X,\rho]]dt. \tag{1.27}$$

It is to be noted that the density matrix in the above equation represents a state averaged over all possible measurement results(which have been ignored).

1.2 Brief Review of Quantum Optics

In this section I review the essential concepts of quantum optics, that would help make the thesis self contained. The classical field equations of electromagnetism are a good starting point for the quantization of the electromagnetic field-light. Consider a classical electromagnetic field in empty space in the absence of any sources such as currents are charges. This free electromagnetic field obeys the celebrated Maxwell equations

$$\nabla \cdot \vec{E} = 0 \tag{1.28}$$

$$\nabla \cdot \vec{B} = 0 \tag{1.29}$$

$$\nabla \times \vec{E} = -\frac{\partial \vec{B}}{\partial t} \tag{1.30}$$

$$\nabla \times \vec{B} = \frac{1}{c^2}\frac{\partial \vec{E}}{\partial t} \tag{1.31}$$

In the absence of sources, the electromagnetic field in gauge invariant. This invariance allows us to choose the vector potential $\vec{A}(\vec{r},t)$ in a way that the Coulomb condition

$$\nabla \cdot \vec{A} = 0 \tag{1.32}$$

is satisfied. In terms of $\vec{A}(\vec{r},t)$, the electric and magnetic fields are

$$\vec{E} = \frac{\partial \vec{A}}{\partial t} \tag{1.33}$$

$$\vec{B} = \nabla \times \vec{A}. \tag{1.34}$$

Using Eq. (1.34) along with Eq. (1.32) in Eq. (1.31) we get a wave equation for $\vec{A}(\vec{r},t)$,

$$\nabla^2 \vec{A}(\vec{r},t) = \frac{1}{c^2}\frac{\partial^2 \vec{A}}{\partial^2 t}. \tag{1.35}$$

Separating the vector potential into two complex terms and restricting the field to a finite volume of space, we can Fourier expand the vector potential in terms of discrete set of orthogonal mode functions $\vec{u}_k(\vec{r})$ as,

$$\vec{A}(\vec{r},t) = \sum_k c_k \vec{u}_k(\vec{r}) e^{-i\omega_k t} + \sum_k c_k^\dagger \vec{u}_k^*(\vec{r}) e^{i\omega_k t}, \tag{1.36}$$

where the Fourier coefficients c_k and $c_k^\dagger$ are constant for a free field. Further since the vector potential satisfied the homogeneous wave equation 1.35, we immediately get using 1.36,

$$(\nabla^2 + \frac{\omega_k^2}{c^2})\vec{u}_k(\vec{r}) = 0 \tag{1.37}$$

The mode functions $\vec{u}_k$ are also required to satisfy the gauge condition 1.32 and leading to

$$\nabla \cdot \vec{u}_k(\vec{r}) = 0. \tag{1.38}$$

The mode functions depend on the boundary conditions of the physical volume under consideration. For a cube of side L, we can write $\vec{u}_k(\vec{r})$ as

$$\vec{u}_k(\vec{r}) = \frac{1}{L^{3/2}}\hat{\epsilon}^{(\lambda)}e^{i\vec{k}.\vec{r}}, \tag{1.39}$$

where $\hat{\epsilon}^{(\lambda)}$ is the unit polarization vector and is required to be perpendicular to $\vec{k}$. The components of $\vec{k}$ take the values

$$k_x = \frac{2\pi n_x}{L}, n_x = 0, \pm 1, \pm 2, \pm 3, \ldots \tag{1.40}$$

$$k_y = \frac{2\pi n_y}{L}, n_y = 0, \pm 1, \pm 2, \pm 3, \ldots \tag{1.41}$$

$$k_z = \frac{2\pi n_z}{L}, n_z = 0, \pm 1, \pm 2, \pm 3, \ldots \tag{1.42}$$

Thus the vector potential may now be written as,

$$\vec{A}(\vec{r}, t) = \sum_k \left(\frac{\hbar}{2\omega_k \epsilon_0}\right)^{1/2} [a_k \vec{u}_k(\vec{r})e^{-i\omega_k t} + a_k^\dagger \vec{u}_k^*(\vec{r})e^{i\omega_k t}] \tag{1.43}$$

where the normalization factors have been chosen such that the amplitudes a_k and $a_k^\dagger$ are dimensionless and the corresponding electric field is

$$\vec{E}(\vec{r}, t) = i\sum_k \left(\frac{\hbar\omega_k}{2\epsilon_0}\right)^{1/2} [a_k \vec{u}_k(\vec{r})e^{-i\omega_k t} - a_k^\dagger \vec{u}_k^*(\vec{r})e^{i\omega_k t}] \tag{1.44}$$

In the classical electromagnetism theory these Fourier amplitudes are complex numbers. Quantization of the electromagnetic field is accomplished by choosing a_k and $a_k^\dagger$ to be

mutually adjoint operators obeying the commutation relations

$$[\hat{a}_k, \hat{a}_{k'}] = [\hat{a}_k^\dagger, \hat{a}_{k'}^\dagger] = 0 \text{ and } [\hat{a}_k, \hat{a}_{k'}^\dagger] = \delta_{kk'}. \tag{1.45}$$

These operators are also called as creation and annihilation operators for the reasons we shall describe in the next section. The ensemble of independent harmonic oscillators obeying the above relations describes the dynamical behavior of the electric-field amplitudes. The Hamiltonian of the field then is given as,

$$H = \frac{1}{2}\int_{L^3}\left[\epsilon_0 \vec{E}^2 + \frac{1}{\mu_o}\vec{B}^2\right] d^3r = \sum_k \hbar\omega_k \left(\hat{a}_k^\dagger \hat{a}_k + \frac{1}{2}\right) \tag{1.46}$$

where the summation represents the discrete nature of quantum mechanics and the Hamiltonian has the familiar form of the harmonic oscillator. In quantum mechanics, the allowed physical states for system with the Hamiltonian are the eigen states of $\hat{H}$, where the operator $\hat{H}$ represents the Hamiltonian operator.

1.2.1 Fock States

In the case for the electromagnetic field the energy eigen states would be the photon number states and are also called as Fock-states. The energy of a single photon in a mode of frequency ω is given as $E = \hbar\omega$. If we measure the energy of a particular mode, we expect the combined energy of all the photons. Thus the measurement of energy is equivalent to counting the number of photons in a particular mode. The observables in quantum mechanics are represented by the Hermitian operators. Thus the operator $\hat{n} = \hat{a}^\dagger\hat{a}$, is known as the photon number operator and its eigenstates are $|n\rangle$ and are called as Fock states after the Russian physicist V. A. Fock. Therefore we have,

$$\hat{n}\,|n\rangle = n\,|n\rangle \qquad\qquad (n = 0, 1, 2, 3, \ldots)\,. \tag{1.47}$$

Fock states $\{|n\rangle\}$ are orthonormal

$$\langle m|n\rangle = \delta_{nm} \tag{1.48}$$

and form a complete set

$$\sum_{n=0}^{\infty} |n\rangle \langle n| = 1, \tag{1.49}$$

thereby serving as a basis for the representation of arbitrary states and operators.

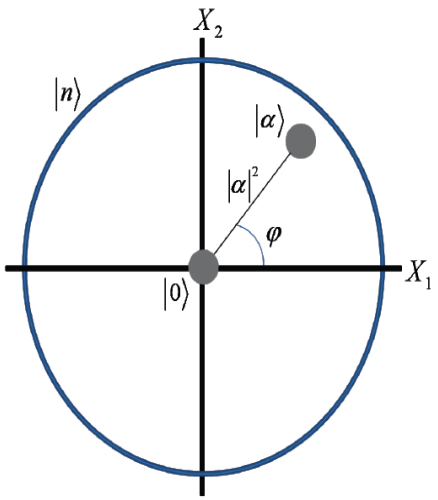

FIGURE 1.2. Phase space depiction quantum states. The vacuum state $|0\rangle$ contains an equal uncertainty in both $\mathbf{X_1}$ and the $\mathbf{X_2}$ quadrature. The coherent state $|\alpha\rangle$ is a displaced vacuum state with amplitude $|\alpha|^2$ and phase φ. A number state $|n\rangle$ is depicted as a circle contaning a known number of photons, but having a completely uncertain phase distribution.

One of the most intuitive ways to view the Fock states, which are states of electromagnetic field is to look at its phase space diagram. This is a simple pictorial view of what we will see are the dimensionless position and momentum of the state of the electromagnetic field. The phase space diagram pictorially shows the uncertainty a given state has in the two quadratures depicted. The uncertainty principle requires that the uncertainty in both quadratures obeys the inequality $\langle(\Delta\hat{X}_1)^2\rangle\langle(\Delta\hat{X}_2)^2\rangle \geq 1/16$. A minimum uncertainty state is a state whose uncertainty is such that the equality holds. The vacuum state $|0\rangle$ is a such a state that the equality holds. The vacuum state $|0\rangle$ is a minimum uncertainty state about the center the phase space diagram, with quadrature uncertainties $\langle(\Delta\hat{X}_1)^2\rangle = \langle(\Delta\hat{X}_2)^2\rangle = 1/4$. It contains equal uncertainty in both quadratures, and is thus depicted as a filled in circle at the center. The most classical state of light, the coherent state $|\alpha\rangle$, is also a minimum uncertainty state with the equality satisfying. This

is because, a coherent state $|\alpha\rangle$ can be generated by displacing vacuum and the corresponding displacement operator is $\hat{D}(\alpha) \equiv e^{\alpha\hat{a}^\dagger - \alpha^*\hat{a}}$. That is to say that the coherent state is displaced vacuum with an amplitude $|\alpha|^2$ and phase ϕ. On the other hand number states $|n\rangle$ is a state that contains a perfectly well-defined number of photons, but contains completely uncertain phase. These phase space diagrams for these states are shown in Fig. 1.2.There is an another class of states called as phase states which I shall discuss later in the chapter.

The operators $\hat{a}$ and $\hat{a}^\dagger$ act on the energy eigenstates as

$$\hat{a}\,|n\rangle = \sqrt{n}\,|n-1\rangle\,, \tag{1.50}$$

$$\hat{a}^\dagger\,|n\rangle = \sqrt{n+1}\,|n+1\rangle\,. \tag{1.51}$$

From the above relations it can be seen that the *annihilation operator* $\hat{a}$ takes a photon out of the field implying that a process involving absorption can be modeled as a function of $\hat{a}$. On the other hand a *creation operator*, $\hat{a}^\dagger$ adds energy to the field by creating a photon.

1.2.2 Description of Phase

In this section I shall discuss the *optical phase* and various attempts to define a phase operator. For a monochromatic electromagnetic field propagating in the $\mathbf{k}$ direction, we can express the electric field as

$$\mathbf{E}(\mathbf{r},t) = E_0 \sin(\mathbf{k}.\mathbf{r} - \omega t + \phi) \tag{1.52}$$

where E_0 is the amplitude and ϕ is the phase. The phase is just a real number but cannot be measured directly and should be determined from the variation of $E(r,t)$. Dirac [1] first wrote the phase operator as,

$$\hat{a} = e^{i\hat{\phi}}\sqrt{\hat{N}}. \tag{1.53}$$

Note the phase is now written as an operator in the exponent. In his paper, Dirac considered the number and phase operators as conjugate variable which allows to write the

commutation relation

$$\left[\hat{N}, \hat{\phi}\right] = i. \tag{1.54}$$

However the above two definitions have problem associated. In Eq. (1.53), the phase operator is not hermitian and in quantum mechanics, we wish to represent the observables by Hermitian operators since the eigen values of Hermitian operators are real and would correspond to the actual outcome of measurement. The commutator relation in Eq. (1.54) is not properly defined in the number state basis. If we evaluate the expectation of the commutator in Eq. (1.54) we get,

$$\begin{aligned} \langle n'[\hat{N}, \hat{\phi}]n\rangle &= i\langle n'|n\rangle \\ \langle n'|\hat{N}\hat{\phi}|n\rangle - \langle n'|\hat{\phi}\hat{N}|n\rangle &= i\delta_{n'n} \\ (n'-n)\langle n'|\hat{\phi}|n\rangle &= i\delta_{n'n} \end{aligned} \tag{1.55}$$

which indicates that one cannot define the matrix elements for the phase operator defined in Eq. (1.53) in the Fock basis.

For non-commuting observables such as $\hat{N}$ and $\hat{\phi}$ there exists the Heisenberg uncertainty relation first given by Dirac [1],

$$\Delta N \Delta\phi \geq 1. \tag{1.56}$$

In the light of Eq. (1.55), this uncertainty relation does not necessarily be implied by the commutator in Eq. (1.54), but can be naively derived from the Energy-Time uncertainty relation

$$\Delta E \Delta t \geq \hbar. \tag{1.57}$$

For a monochromatic standing wave of frequency ω and with an average n number of photons, we get the total energy $E = n\hbar\omega$. Due to the absence of propagation, the phase $\phi = \omega t$ at any given time. Keeping ω a constant due to the monochomaticity, the fluctuations in energy is $\Delta E = \hbar\omega\Delta n$ and the fluctuations in phase $\Delta\phi = \omega\Delta t$.

Using these two results in Eq. (1.57) we get the number-phase uncertainty relation as in Eq. (1.56).

A resolution of the problem associated with the commutator Eq. (1.54) was proposed by Louisell [16] and was later developed by Susskind-Glogower [17]. They pointed out that although it is not possible to define a Hermitian phase operator, it is possible to define a Hermitian sine and cosine operators that give valid uncertainty relations. These sine and cosine operators satisfy the following commutation relations

$$\left[\widehat{\cos\phi}, \hat{N}\right] = i\widehat{\sin\phi} \tag{1.58}$$

$$\left[\widehat{\sin\phi}, \hat{N}\right] = -i\widehat{\cos\phi} \tag{1.59}$$

and the corresponding uncertainty relations

$$\Delta N \Delta \cos\phi \geq |\langle\widehat{\sin\phi}\rangle| \tag{1.60}$$

$$\Delta N \Delta \sin\phi \geq |\langle\widehat{\cos\phi}\rangle|. \tag{1.61}$$

We can see that for small ϕ is gives back the Eq. (1.56), while still these are not strictly phase operators. Further, it was pointed out in Ref. [18, 19] that these phase operators do not allow existence of a unique Hermitian phase operator.

Another approach to finding a Hermitian phase operator is the Pegg-Barnett formalism [20, 21, 22]. The make use of what is called as phase states. The basis of this formalism is to put an upper limit s on the photon number, then take the limit as s tends to infinity.Consider the state $|\phi_m\rangle$ defined on a finite Fock basis by

$$|\phi_m\rangle = (s+1)^{-1/2} \sum_{n=0}^{s} e^{in\phi_m} |n\rangle , \tag{1.62}$$

where

$$\phi_m = \phi_0 + \frac{2\pi m}{s+1}; m = 0, 1, \ldots, s \tag{1.63}$$

and ϕ_0 is an arbitrary constant. These states form a complete orthonormal set on the truncated $(s+1)$ dimensional Hilbert space. The Pegg-Barnett Hermitian phase operator

is defined as

$$\hat{\phi}_s = \sum_{m=0}^{s} \phi_m \left|\phi_m\right\rangle \left\langle\phi_m\right| . \tag{1.64}$$

For states restricted to the truncated Hilbert space the measurement statistics of ϕ are given by the discrete distribution

$$P_m = |\langle\phi_m|\psi\rangle_s|^2 \tag{1.65}$$

where $|\psi\rangle_s$ is any state defined on the truncate Fock-basis. In the Pegg-Barnett formalism, the limit of $s \to \infty$ is taken after expectation values have been determined. This leads to the probability density $P(\phi)$ as,

$$P(\phi) = lim_{s\to\infty}\left[\left(\frac{2\pi}{s+1}\right)^{-1} P_m\right] = \frac{1}{2\pi}\left|\sum_{n=0}^{\infty} e^{in\phi}\psi_n\right|^2 \tag{1.66}$$

where

$$\psi_n = \langle n|\psi\rangle_s; \phi = lim_{s\to\infty}\frac{2\pi m}{s+1}.$$

This convergence in distribution ensures that the moments of the Pegg-Barnett Hermitain phase operator converge as $s \to \infty$, to the moments of the phase probability density.

In essence Pegg-Barnett formalism is a phase state projector. Although it seems that the problem started with Dirac would be concluded with the Pegg-Barnett formalism, it is to be noted that the phase states are not physical states [23] and so simulating a Phase operator may not be trivial.

1.2.3 Phase Estimation

Unlike most other quantities that we would wish to measure, it is not possible to measure phase directly. In order to perform a *phase measurement*, we need to implement the Hermitian phase operator as in Eq. (1.64). It turns out that this is not a trivial problem and is still an open question.

On the other hand, as described at the beginning of this subsection, one can always *estimate an unknown phase*from measurement of intensity or the photon number of the ra-

diation mode in the question. An intensity measurement would correspond to the classical case in the sense that we can approximate the analytically treatment of the measurement based on the wave nature of radiation. In contrast a photon number measurement is obviously a quantum version of the detection.

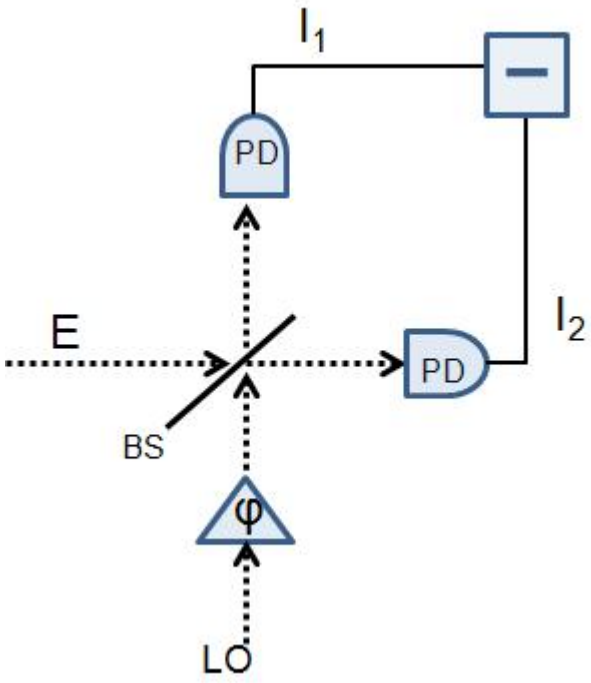

FIGURE 1.3. Schematic of balanced homodyne detection. Here E corresponds to the electric field of the input radiation, LO: local oscillator, BS:beam splitter, PD: photodetector.

The standard technique to measure the phase difference is using what is called as homodyne detection as shown in Fig. 1.3. A single mode of radiation $\vec{E}$ with an unknown phase is input on a 50-50 beam splitter. At the other input of the beam splitter a strong local oscillator such as a laser, $\alpha e^{i\phi}$ where $|\alpha|^2 << 1$ is incident. The known phase ϕ in the figure establishes a phase difference between the two input modes. By detecting the difference of intensities at the output modes $I_1 - I_2$, one can measure the phase of the unknown signal. One can improve upon this by adjusting the phase of the local oscillator by some adaptive techniques as in Ref. [24].

Another approach is to perform interferometric phase measurements where instead of measuring the phase of a single mode and assuming that the local oscillator field is sufficiently intense so that it can be treated classically, we are measuring the phase difference between two modes both of which are treated quantum mechanically.

Typically to achieve this task one uses Mach-Zehender interferometer which can be treated as an extension of the balanced homodyne detection scheme depicted in Fig. 1.3 where we use an extra beam splitter at the input mode. The schematic is shown in Fig.1.4. Two input modes are combined at a beam splitter, after which one of the mode is subjected to the phase shift with respect to the other mode and then the two modes are recombined at a second beam splitter.

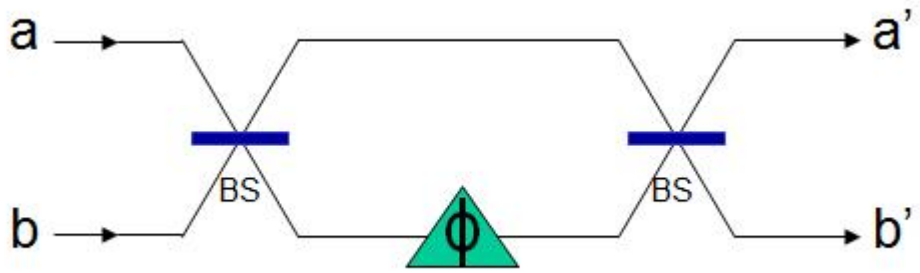

FIGURE 1.4. Mach-Zehender interferometer setup. The input modes enter at **a** and **b** and combine at the beam splitter. The phase difference between the modes is encoded in ϕ. The modes are then recombined at the second beams plitter and are propagated as modes **a'** and **b'**

By using another beam splitter we can establish the quantum-correlations between the modes. The drastic non-classicality here is due to the famous Hong-Ou-Mandel effect [25], where if two single photons are incident on a beam splitter then at the output mode both either exit port 1 or port 2. This kind of bunching could be understood due to the bosonic nature of the photons.

Quantum correlations have been proven to increase the precision of the phase estimate, but in general it is much easier to produce input states without quantum correlations between the modes, which is usually accomplished by the first beam splitter. In standard

interferometry, an experimenter would have control over the input state and the detection strategy at the output towards precise estimation of the phase.

The phase estimate that is being discussed here is the phase uncertainty $\Delta\phi$. If we have a probability density, $P(\phi)$ then we can use

$$\Delta\phi^2 = \langle\phi^2\rangle - \langle\phi\rangle^2. \tag{1.67}$$

For most of the interferometric detection schemes, to be discussed later, we do not have a probability density $P(\phi)$ but just the clicks at the photo detectors. Alternatively the estimate is the signal to noise ratio, and quantum mechanically given as

$$\Delta\phi = \frac{\Delta\hat{A}}{|\frac{\partial\langle\hat{A}\rangle}{\partial\phi}|}, \tag{1.68}$$

where $\hat{A}$ is an observable corresponding to the output detection scheme. It is well known that if we feed a state with a mean photon number of $\overline{n}$ into one arm of the interferometer and vacuum at the other port, we can obtain a phase estimate as $1/\sqrt{\overline{n}}$. It has also been found that no matter what state we use at the one of the input, as long as the second input of the interferometer is maintained at vacuum the phase estimate has a lower bound of $1/\sqrt{\overline{n}}$. This limit is called as shot-noise limit and is a consequence of the vacuum fluctuations. The most standard operation in laboratory is to use the laser as one of the input and vacuum as the other input of the interferometer.

On contrary there are several proposals for reducing the phase estimate to $1/\overline{n}$ which is called as Heisenberg limit in light of the number phase uncertainty relation Eq. (1.56). The first of these proposals was due to Caves [3], where he suggested using coherent laser light at port **a** and squeezed vacuum at port **b** and detect the photon number difference at the output ports **a'** and **b'** of the interferometer shown in Fig. 1.4. For the right squeezing parameter these measurements give an Heisenberg-limited phase estimate.

As discussed earlier, an experimenter would have choice over the input state and the detection strategy that could be built. The most widely used one is the photon difference

measurement at the output [3, 26, 27, 4, 28]. Another detection scheme called as an optimal detection scheme was proposed by Sanders and Milburn [29], and has been shown, that it can be approximately implemented using adaptive measurement techniques [30, 31]. Berry and Wiseman also have analytically derived the so called optimal state which is the best state in the utility of the measurement scheme proposed by Sanders and Milburn.

Considering the interferometer in Fig. 1.4, the role of the first beam splitter is to establish quantum correlations between the internal modes. These correlations not necessarily be preserved if there is some kind of interaction with external environment along the path to the second beam splitter. The process of decoherence where the quantum properties or more precisely quantum correlations are disturbed. Under such conditions it is extremely challenging to get a better phase estimate. A number of authors have attempted to study the interferometric phase measurements in presence of decoherence [32, 33, 34]

In this thesis I will consider "Parity Detection" for a class of states in the next chapter and show that this detection would in deed unify all the existing measurement schemes. Later, I shall consider the optimal measurement scheme proposed in Ref. [29] with photon-loss, in which I shall present the full density matrix calculations. This is required because a pure state after loosing a photon over which we do not have any further control, the state becomes mixed and should be dealt as a density matrix.

2 Parity Measurements in Quantum Optical Metrology

2.1 Introduction

In this chapter, I consider the interferometry with the parity detection scheme for several class of states which have been shown to attain sub-shot noise limited phase estimate with respective detection schemes. In this chapter we show that parity detection scheme unifies all the detection strategies. At the time of writing this thesis, the ongoing research in our group at LSU shows that one can achieve *" Sub-Heisenberg limited"* phase estimate using parity detection with squeezed light at the input of the interferometer.

Quantum optical metrology deals with the estimation of an unknown phase by exploiting the quantum nature of the input state under consideration [35, 36, 37, 38, 39, 40, 41, 42, 43, 44, 45, 46, 47, 26, 4, 27, 48, 49, 50, 51, 30, 52, 53, 54, 34]. Due to the inherent uncertainty imposed by quantum mechanics, the problem reduces to minimizing the uncertainty of the expectation value of a suitable observable. In the usual classical setting, for a given mean number of input photons, N, the phase estimate scales as $1/\sqrt{N}$, which is usually referred as shot-noise limit (SL). It has been shown that by exploiting the signature quantum properties such as entanglement the uncertainty can be reduced to the Heisenberg limit (HL) of $1/N$; an enhancement of a factor of $\sqrt{N}$. Achieving a sub-shot noise limit or the HL depends on the nature of the input states and the detection strategy of the output measurement [48, 49, 50, 51, 30, 52, 53, 54, 34].

Precise optical phase measurement has been an open problem for many years and has many applications, most notable of them being to gravitational wave detection [3, 55]. Phase measurements can be efficiently implemented by the Mach-Zehender interferometer (MZI) shown in Fig. 2.1. It has been shown that using NOON states *within* the interferom-

eter, one can achieve the exact Heisenberg Limit [4, 29, 56, 57, 58, 59, 60, 61, 62, 63, 32, 64]. NOON states are similar to maximally entangled states first proposed by Bollinger *et. al* [37] in the context of frequency metrology using trapped ions. Formally, in the present context of phase measurement, considering the MZI shown in Fig. 2.1, the NOON states are written as:

$$|\psi\rangle_N = \frac{|N\rangle_{a'}|0\rangle_{b'} + |0\rangle_{a'}|N\rangle_{b'}}{\sqrt{2}}. \tag{2.1}$$

The most simple approach in phase estimation one wishes to take, is to fix the detection strategy, i.e. to fix a particular phase dependent observable at the output and look for the behavior of the input states. While a detection of the signal is done at the output ports, one can always transform the observable through the beam splitter and can think of the detection *within* the interferometer. Obviously, both descriptions are equivalent but the latter may help in understanding the direct effect of the measurement on the states after acquiring the phase shift.

Various measurement schemes have been shown to surpass the SL. Yurke *et al.* [26] have shown that by using the output photon difference, for the input state $[|N/2\rangle_a|N/2\rangle_b + |(N+1)/2\rangle_a|(N-1)/2\rangle_b]/\sqrt{2}$, a minimum phase sensitivity of $2/N$ can be achieved. Sanders and Milburn have computed the optimal measurement [49], written as Positive Operator Valued Measure (POVM) [65], to achieve the HL. The method specified by Sanders and Milburn is independent of the system phase and thus an optimal one. Berry and Wiseman [30] have considered the optimal POVM and derived the optimal input state to achieve the minimum uncertainty that scales as the HL. They also showed a way of approximately implementing the optimal POVM using a feedback technique. With this feedback technique along with the Kitaev algorithm for phase estimation [10], Higgins *et al.* have experimentally achieved the HL scaling of the optical phase measurement [66]. In this chapter, we will discuss the parity measurement, which detects whether the number of photons in a given output mode is even or odd so treating the interferometer phase as

local phase is enough which can be estimated using the linear error propagation formula (See Eq. (2.4) in Sec.2.2).

As we make extensive use of the Schwinger representation to analyze the MZI, we wish to present a brief discussion of the representation. Any four-port optical lossless device, such as the MZI considered here, can be conveniently described using the Schwinger representation of the angular momentum [49, 51]. The operators, which form an SU(2) rotation group, and describe the MZI [65] are: $\hat{J}_x = (\hat{a}^\dagger\hat{b}+\hat{a}\hat{b}^\dagger)/2$, $\hat{J}_y = (\hat{a}^\dagger\hat{b}-\hat{a}\hat{b}^\dagger)/2i$, $\hat{J}_z = (\hat{a}^\dagger\hat{a} - \hat{b}^\dagger\hat{b})/2$, where $\hat{a}$ and $\hat{b}$ are the mode operators which obey bosonic commutation relation, $[\hat{a}, \hat{a}^\dagger] = [\hat{b}, \hat{b}^\dagger] = 1$. The angular momentum operators obey $[\hat{J}_i, \hat{J}_j] = i\epsilon_{ijk}\hat{J}_k$. The total photon number is $\hat{N} = \hat{a}^\dagger\hat{a} + \hat{b}^\dagger\hat{b}$, and $\hat{J}^2 = \hat{J}_x^2 + \hat{J}_y^2 + \hat{J}_z^2 = (\hat{N}/2)(\hat{N}/2+1)$ is the Casimir invariant. The generator for beam-splitter transformation is usually represented by $\hat{J}_x$ [49]. The combined two mode input state is represented by the simultaneous eigen state of $\hat{J}^2$ and $\hat{J}_z$, i.e $|j\mu\rangle_z$, where $|j+\mu\rangle$ and $|j-\mu\rangle$ represent $|N\rangle_a$ and $|N\rangle_b$ respectively and $j = N/2$ for a fixed input photon number N. Correspondingly, if $|j\nu\rangle_z$ represents the output state, then ν represents the output photon number difference, $(N_a - N_b)|_{out}$. In this representation the Mach Zehender Interferometer is given by an operator, $\hat{\mathcal{I}} = \exp(-i\varphi\hat{J}_y)$. For a given input state $|j\mu\rangle$, the output state can be written as, $\hat{\mathcal{I}}\,|j\mu\rangle = e^{-i\varphi\hat{J}_y}\,|j\mu\rangle = \sum_{\nu=-j}^{j} d^j_{\nu,\mu}(\varphi)\,|j\nu\rangle$, where $d^j_{\nu,\mu}(\varphi)$ is the usual rotation matrix elements [67, 68].

This chapter is organized as follows. In section 2.2 we discuss the parity measurement and setup a general framework of calculating the expectation value for an arbitrary input state. In section 2.3 we apply it to specific input states including a combination of a NOON state and a dual-Fock state, followed by section 4.4 with conclusions.

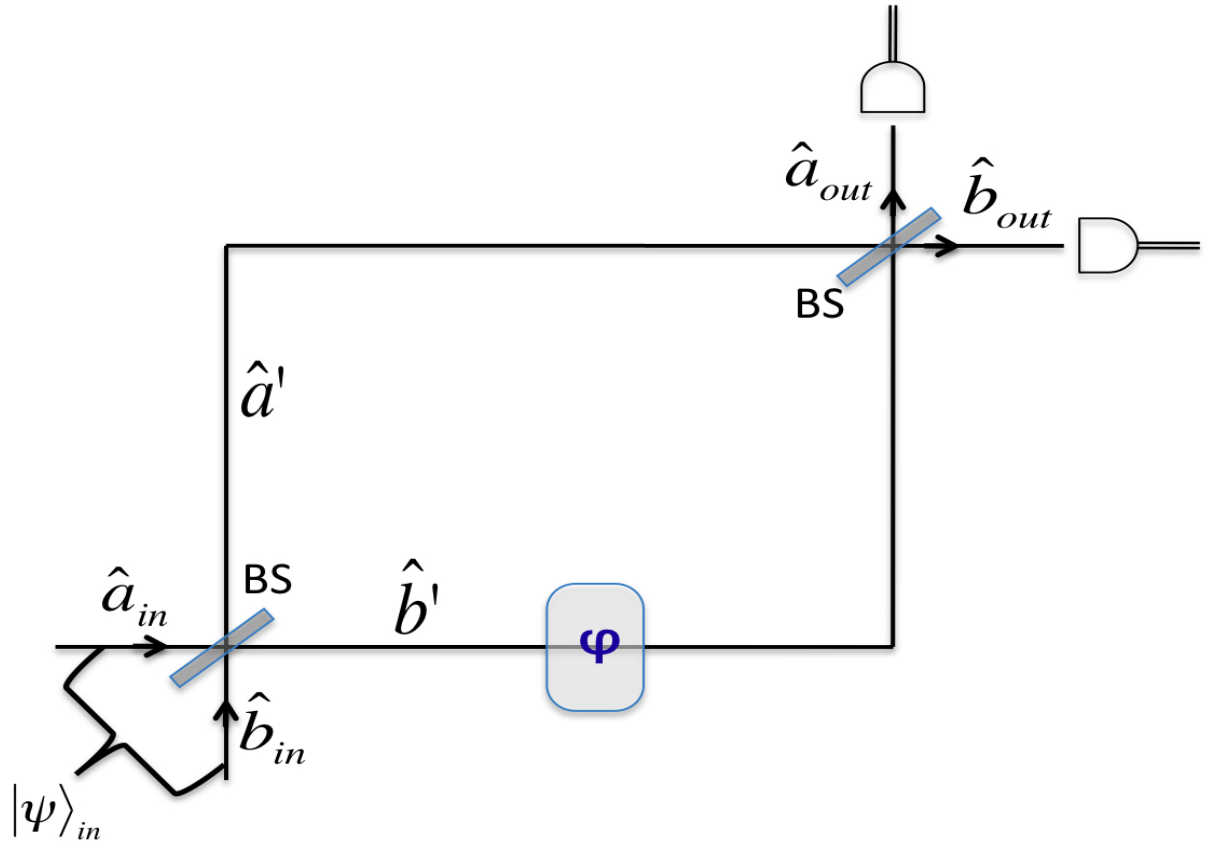

FIGURE 2.1. Schematic of a Mach-Zehender Interferometer (MZI). $|\psi\rangle_{in}$ represents the joint input state at $\hat{a}_{in}$ and $\hat{b}_{in}$.The photon number states entering at $\hat{a}_{in}, (\hat{b}_{in})$ are $|N\rangle_a(|N\rangle_b)$. The symbol φ represents the relative phase between the modes, within the interferometer. BS: Beam Splitter.

2.2 Parity Detection

Parity detection was first proposed by Bollinger *et al.* in 1996 to study spectroscopy with a "maximally entangled" state of trapped ions [37]. The detection considered there is $(-1)^{\hat{N}_e}$, where $|N\rangle_e$ represents N atoms in excited state. It is straightforward to draw the parallel between the two level atom and the MZI depicted in Fig. 2.1. Thus in the case of the optical phase measurements, we have the $|\psi\rangle_n$ is the maximally entangled and the detection operator which was first proposed by Gerry [39]:

$$\hat{P} = (-1)^{\hat{b}^{\dagger}_{out}\hat{b}_{out}} = (-1)^{j-\hat{J}_z}. \tag{2.2}$$

There is no particular reason to perform such a detection on $\hat{b}_{out}$ and choosing $\hat{a}_{out}$ works equally well. Gerry and Campos have applied this operation to interferometry with NOON states, resulting in the exact HL [57]. As stated in the introduction, these states are not the input states of the MZI, but are states *after* the first BS. One can quite easily write down the input state using a beam splitter transformation as we will do it now. In the Schwinger representation, the NOON states is represented as: $|\psi\rangle_N = (|j,j\rangle + |j,-j\rangle)/\sqrt{2}$. Denoting the BS with $\hat{J}_x$, we get

$$|\psi\rangle_i = e^{-i\frac{\pi}{2}\hat{J}_x} |\psi\rangle_N = \sum_{\mu=-j}^{j} A_\mu |j,\mu\rangle , \tag{2.3}$$

where the amplitude,

$$A_\mu = \frac{1}{\sqrt{2}} \left[e^{i(\mu-j)\pi/2} d^j_{\mu,j}(\frac{\pi}{2}) + e^{i(\mu+j)\pi/2} d^j_{\mu,-j}(\frac{\pi}{2}) \right] .$$

We used $e^{-i\frac{\pi}{2}\hat{J}_x} = e^{i\frac{\pi}{2}\hat{J}_z} e^{-i\frac{\pi}{2}\hat{J}_y} e^{-i\frac{\pi}{2}\hat{J}_z}$ in obtaining the above result. Thus $|\psi\rangle_i$ is the input state of the MZI to get the exact HL with parity detection. The coefficients are plotted in Fig. 2.2.

Recently, Uys and Meystre [44] noted that a state whose coefficients look alike the coefficients plotted in Fig. 2.2 also gives an exact Heisenberg limit. They obtained this result via numerical simulations and an explicit mathematical expression was not given. From Fig. 2.2 it appears that the state obtained in Ref. [44] is a beam splitter transformation of the NOON state which is given by Eq. (2.3).

The phase uncertainty is typically given as [65]:

$$\delta\varphi = \frac{\Delta\hat{P}}{|\partial_\varphi \langle\hat{P}\rangle|}, \tag{2.4}$$

where $\Delta\hat{P} = \sqrt{\langle\hat{P}^2\rangle - \langle\hat{P}\rangle^2} = \sqrt{1 - \langle\hat{P}\rangle^2}$, since $\hat{P}^2 = 1$.

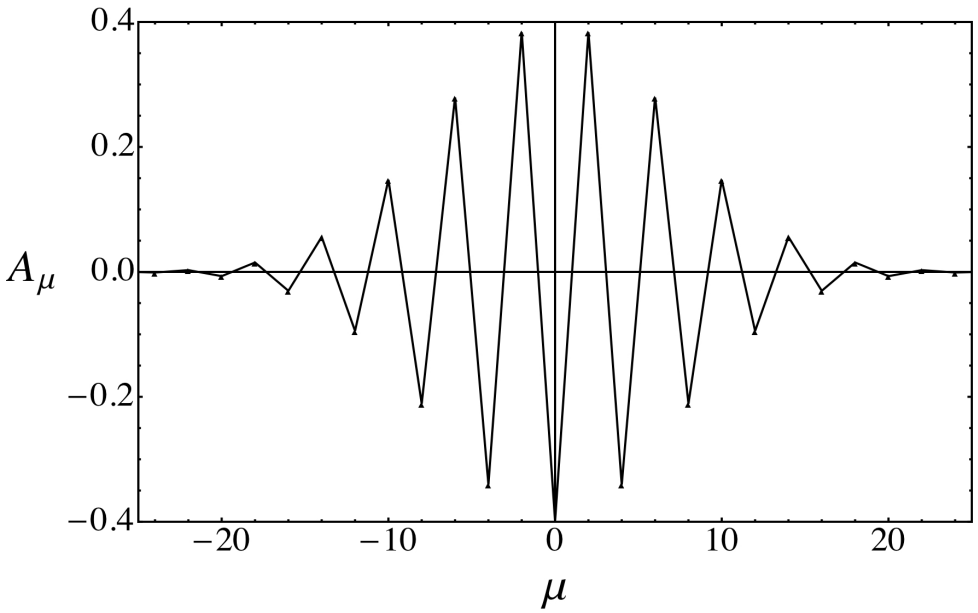

FIGURE 2.2. The coefficients of the state given in Eq. (2.3) for an input photon number, N=100. This is the input state to the MZI shown in Fig. 2.1 such that it is NOON state (*after the first beam splitter*) and thereby giving the Heisenberg-limited phase estimate.

We can obtain more insight on $\hat{P}$ by transforming through the BS and further express it as a projection operator by using the completeness relation:

$$\begin{aligned}\hat{Q} &= e^{-i\frac{\pi}{2}\hat{J}_x}\hat{P}e^{i\frac{\pi}{2}\hat{J}_x} = (-1)^j e^{i\pi\hat{J}_y} \\ &= \sum_{\nu,\mu=-j}^{j}(-1)^j d^j_{\nu,\mu}(-\pi)|j\nu\rangle\langle j\mu|. \end{aligned} \tag{2.5}$$

It is straight forward to see that $\hat{Q}^2 = 1$. Using the relations in Ref. [67] and noting $d^j_{\nu,\mu}(-\pi) = (-1)^{2\nu}\delta_{\nu,-\mu}$, we get

$$\hat{Q} = i^N \sum_{k=0}^{N}(-1)^k |k, N-k\rangle\langle N-k, k|. \tag{2.6}$$

If the NOON states are under consideration for the above expression of the observable $\hat{Q}$, the only relevant terms would be for $k = 0$ and $k = N$. Thus the observable considered in Refs. [4, 32] is: $\hat{Q}_N = |0, N\rangle\langle N, 0| + |N, 0\rangle\langle 0, N|$, that leads to the HL for NOON states. This gives the same expectation value, and thus $\hat{Q}_N$ can be implemented with parity detection for the NOON states. Explicitly, after the phase shifter, $|\psi\rangle_N$ becomes:

$|\psi\rangle_{N,\varphi} = |N,0\rangle + e^{iN\varphi}\,|0,N\rangle$, which leads to (see also Ref. [69]):

$$\langle\psi|\,\hat{Q}\,|\psi\rangle_{N,\varphi} = \begin{cases} i^{N+1}\sin N\varphi, & N \text{ odd}, \\ i^{N}\cos N\varphi, & N \text{ even}. \end{cases} \tag{2.7}$$

Using Eq. (2.7) in Eq. (2.4) we immediately get $\delta\varphi = 1/N$.

Now we shall obtain the expectation value of parity observable for an arbitrary input state. In the Schwinger notation an arbitrary two-mode input and the corresponding output states are written as,

$$|\psi\rangle_{\text{in}} = \sum_{2j=0}^{\infty}\sum_{\mu=-j}^{j}\psi_{\mu,j}\,|j,\mu\rangle\,, \tag{2.8}$$

$$|\psi\rangle_{\text{out}} = \hat{\mathcal{I}}\,|\psi\rangle_{\text{in}} = \sum_{2j=0}^{\infty}\sum_{\mu=-j}^{j}\psi_{\mu,j}e^{-i\varphi\hat{J}_y}\,|j,\mu\rangle\,, \tag{2.9}$$

where $\psi_{\mu,j}$ is the amplitude for the arbitrary input state. Using the above equation it is straightforward to calculate the expectation value of $\hat{P}$ for an arbitrary input state

$$\begin{aligned}\langle\hat{P}\rangle_{\text{out}} &= {}_{\text{out}}\langle\psi|\hat{P}\,|\psi\rangle_{\text{out}} \\ &= \sum_{2j=0}^{\infty}\sum_{\mu,\mu'=-j}^{j}(-1)^{j-\mu'}\psi^{*}_{\mu',j}\psi_{\mu,j}d^{j}_{\mu'\mu}(2\varphi).\end{aligned} \tag{2.10}$$

The summation over $2j$ describes the situation where the number of photons are not fixed. In what follows we will use a fixed number of input photons N, and this summation will then be dropped. In obtaining the above result, we used: $\langle j'\mu'|\,e^{i\varphi\hat{J}_y}e^{-i\pi\hat{J}_z}e^{-i\varphi\hat{J}_y}\,|j\mu\rangle = \sum_{\nu=-j}^{j}(-1)^{-\nu}d^{j}_{\nu,\mu'}(\varphi)d^{j}_{\nu,\mu}(\varphi)\delta_{j,j'}$.

2.3 Application of the Parity Detection

2.3.1 Parity Detection with Uncorrelated States

We begin with a coherent state input at mode $\hat{a}_{in}$. We have at the input:

$$|\psi\rangle_{\alpha} = \sum_{2j=0}^{\infty}e^{-\frac{|\alpha|^2}{2}}\frac{(\alpha)^{2j}}{\sqrt{(2j)!}}\,|j,j\rangle\,, \tag{2.11}$$

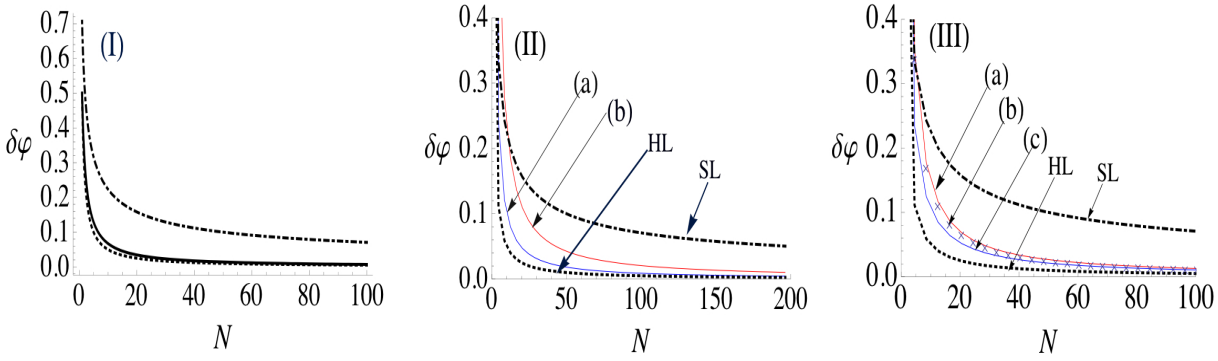

FIGURE 2.3. The variance of $\delta\phi$ versus N. (I) The dual fock state, shown as the continuous curve which is same as given in Ref. [70]. (II) For the combined state $|\psi\rangle_c$, in the absence of relative phase, where (a) $\alpha = \sqrt{\frac{2}{3}}, \beta = \sqrt{\frac{1}{3}}, \theta = 0$, (b) $\alpha = \sqrt{\frac{1}{3}}, \beta = \sqrt{\frac{2}{3}}$ and $\theta = 0$. (III) For a fixed $\alpha = \beta = \frac{1}{\sqrt{2}}$, (a) $\theta = 0$, (b) represented by $\times$ for $\theta = \pi$, (c) $\theta = \frac{\pi}{4}$. In (III) the plots for the case (a) and (b) (represented by $\times$), almost overlap. In all plots the dot-dashed curve is the shot-noise limit (SL) and the dotted curve represents the Heisenberg limit (HL).

where $|\alpha| = \bar{n}$, the average photon number. Using Eq. (2.10), we have:

$$\begin{aligned}\langle \hat{P} \rangle_\alpha &= \sum_{2j=0}^{\infty} e^{-\frac{|\alpha|^2}{2}} \frac{(|\alpha|^2)^{2j}}{(2j)!} d^j_{j,j}(2\varphi) \\ &= \exp\left[-|\alpha|^2 + \frac{|\alpha|^2\sqrt{1+\cos(2\varphi)}}{\sqrt{2}}\right], \end{aligned} \tag{2.12}$$

which, in the limit $\varphi \to 0$, according to Eq. (2.4), immediately leads to $\delta\varphi_\alpha = 1/\sqrt{\bar{n}}$. We thus recover the shot-noise limit. This can also be obtained by $\hat{J}_z$ measurement at the output, which corresponds to the photon number difference. However, in the case of a $\hat{J}_z$ measurement, the shot-noise limit is reached when φ tends to odd multiples of $\pi/2$ [65].

The next simplest uncorrelated state is a number state at $\hat{a}_{in}$ and vacuum at $\hat{b}_{in}$. Thus the input state: $|\psi\rangle_s = |N\rangle_a |0\rangle_b = \sum_{\mu=-j}^{j} \delta_{\mu,j} |j, j\rangle$. The subscript s denotes the input at a single port of MZI. Using Eq. (2.10), we obtain:

$$\langle \hat{P} \rangle_s = \frac{[1+\cos(2\varphi)]^j}{2^j}, \tag{2.13}$$

for which, in the limit $\varphi \to 0$, we get $\delta\varphi_s = 1/\sqrt{2j} = 1/\sqrt{N}$. This result shows that parity detection gives the same result as the $\hat{J}_z$ measurement for a single-port input state [28].

Now we consider the dual-Fock input state. Campos *et al.* have shown the utility of the parity measurements for the dual Fock input state [70]. Their analysis also includes a comparison and contrast of the quantum state distribution with the interferometer with the NOON states (as these are the states within the interferometer). The dual Fock state can be written as: $|\psi\rangle_d = |N, N\rangle = \sum_{\mu=-j}^{j} \delta_{\mu,0} |j\mu\rangle$. Using Eq. (2.10) we immediately get $\langle \hat{P} \rangle_d = (-1)^j d^j_{0,0}(2\varphi)$. Using $\langle \hat{P} \rangle_d$ in Eq. (2.4) for a small phase, $\varphi \to 0$, we get $\delta\varphi_d = 1/\sqrt{2j(j+1)} \propto 1/N$ (see also Ref. [69]). We plot this in Fig. 2.3(I), which is the same as shown in Ref. [70].

2.3.2 Parity Detection with a Combined State

As discussed above, the dual-Fock state and the NOON state, both have an Heisenberg limited phase variance with the parity detection.

It is natural to ask how precisely a state has to be prepared to take the advantage of parity or, in general, any detection scheme. We now attempt to answer this question by considering a combination of a NOON state [see Eq. (2.3)] and a dual-Fock state such as

$$\begin{aligned} |\psi\rangle_{\rm c} &= {\rm C}_N(\alpha |\psi\rangle_i + \beta |\psi\rangle_d) \\ &= {\rm C}_N \left(\alpha \frac{e^{-i\frac{\pi}{2}\hat{J}_x} (|j, j\rangle + |j, -j\rangle)}{\sqrt{2}} + \beta |j, 0\rangle \right). \end{aligned} \tag{2.14}$$

Writing $\alpha = |\alpha| e^{i\theta_\alpha}$ and $\beta = |\beta| e^{i\theta_\beta}$, where the normalization constant is given by

$${\rm C}_N = [1 + 2\sqrt{2}|\alpha||\beta| d^j_{j,0}(\pi/2) \cos(\theta - \frac{N\pi}{4})]^{-\frac{1}{2}}, \tag{2.15}$$

where $\theta = \theta_\alpha - \theta_\beta$ is the relative phase. With such a quantum state as the input of the MZI in Fig. 2.1, we have the output $|\psi\rangle_{\text{c|out}} \equiv \mathcal{I}\,|\psi\rangle_{\text{c}}$. It gives rise to:

$$\begin{aligned}\langle\psi|\,\hat{P}\,|\psi\rangle_{\text{c|out}} = \text{C}_N^2\{|\alpha|^2\langle\hat{P}\rangle_{\text{NOON}} + |\beta|^2\langle\hat{P}\rangle_{\text{dual}} \\ +i^j 2\sqrt{2}|\alpha||\beta|d^j_{0,0}\cos(N\varphi)\cos(\theta)\},\end{aligned} \tag{2.16}$$

where

$$\langle\hat{P}\rangle_{\text{NOON}} = (-1)^j(e^{iN\varphi} + (-1)^N e^{-iN\varphi})/2,$$
$$\langle\hat{P}\rangle_{\text{dual}} = (-1)^j d^j_{0,0}(2\varphi).$$

The above result is obtained using the symmetric properties of the rotation matrix elements listed in Ref. [67] and the Baker-Campbell-Hausdorff (BCH) formula [65]. We can now use this in Eq. (2.4) to calculate $\delta\varphi$. To gain more insight, we will first take $\theta = 0$ and look for the $\delta\varphi$ for various combinations of $|\alpha|$ and $|\beta|$ using $|\alpha|^2 + |\beta|^2 = 1$. The results are shown in the top portion of Fig. 2.3(II).

Next, we fix $|\alpha| = |\beta| = 1/\sqrt{2}$ and vary θ. This is plotted in the in the bottom portion of Fig. 2.3(III). In both the cases we can clearly see that with $|\psi\rangle_{\text{c}}$ at the input, using parity detection, we do get the sub-shot noise limited variance of the optical phase. This result implies a wider applicability of the parity detection.

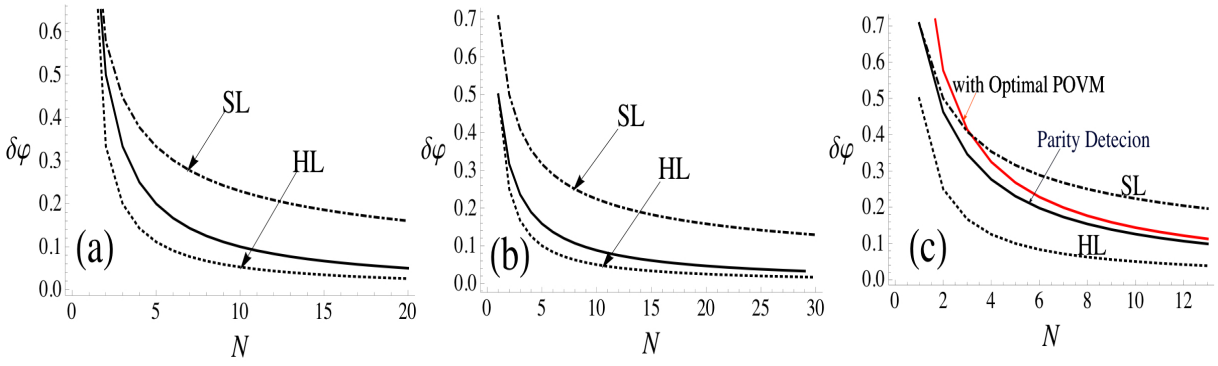

FIGURE 2.4. The variance $\delta\varphi$ for various states. In all the figures, the dotted line corresponds to the Heisenberg limit(HL) and dot-dashed to the shot-noise limit(SL). The continuous line in (a) for the modified-Yuen state, (b) for the $|\psi\rangle_{\text{sp}}$ considered in Ref. [52] and (c) for the optimal state(for comparison $\delta\varphi$ as obtained with[30] optimal POVM is also shown)

2.3.3 Parity Detection with Correlated States

Now we consider a few more quantum-correlated input states for the MZI. Before we begin to explicitly calculate the phase estimate with these states, it is worth pointing out that the primary objective of this paper is to investigate the utility of parity detection scheme and not the role of the quantum correlations-also referred as entaglement-in achieving the sub-shot noise limited phase estimate. The precise question on the role of entanglement in achieving sub-shot noise limited interferometry is beyond the scope of this article.The curious reader may find [71] useful in that direction.

In this section we consider the quantum-correlated states that have been already shown to achieve sub-shot noise limited phase estimate under several different detection schemes. Here we show that all these states does achieve the goal with the parity detection and thus making the parity detection, a unified detection scheme.

Let us begin with the Yurke state discussed in the introduction. In the Schwinger notation it is given as $|\psi\rangle_Y = \sum_{\mu=-j}^{j} \frac{1}{\sqrt{2}}(\delta_{\mu,0} + \delta_{\mu,1}) |j,\mu\rangle$. Using Eq.(2.10) we get the expectation value of parity as [69]:

$$\langle \hat{P} \rangle_Y = \frac{(-1)^j}{2}[d^j_{0,0}(2\varphi) - d^j_{1,1}(2\varphi) + 2d^j_{0,1}(2\varphi)]. \tag{2.17}$$

Again in the limit $\varphi \to 0$, we have using Eq. (2.4) we get: $\delta\varphi \to 1/\sqrt{j(j+1)} \propto \sqrt{2}/N$, which is same as that obtained with the $\hat{J}_z$ measurement [26].

Let us now consider a correlated input state first proposed by Yuen [27]:

$$|\psi\rangle_{\rm yu} = \sum_{\mu=-j}^{j} \frac{1}{\sqrt{2}}(\delta_{\mu,1/2} + i\delta_{\mu,-1/2}) |j,\mu\rangle \,. \tag{2.18}$$

Now by using Eq. (2.4), we get: $\langle \hat{P} \rangle_{\rm yu} = 0$. Thus the parity detection does not give any phase information for the Yuen state. The main reason for the vanishing $\langle \hat{P} \rangle_{\rm yu}$ is the relative phase of $\pi/2$ among the two possible inputs at the MZI. This motivates us to consider the state with zero relative phase, which would be a slightly modified form of

$|\psi\rangle_{\rm yu}$. Let us define the modified Yuen state as,

$$|\psi\rangle_{\rm m.yu} = \sum_{\mu=-j}^{j} \frac{(\delta_{\mu,1/2} + \delta_{\mu,-1/2})}{\sqrt{2}} |j,\mu\rangle \,, \tag{2.19}$$

which then following Eq. (2.10) leads to:

$$\langle \hat{P} \rangle_{\rm m.yu} = i(-1)^j d^j_{\frac{1}{2},-\frac{1}{2}}(2\varphi). \tag{2.20}$$

Thus using Eq. (2.4) one can calculate the variance. In the limit of $\varphi \to 0$ this leads to a sub-shot noise variance as is shown in Fig. 2.4(a).

Berry and Wiseman have proposed the so-called optimal states [30], for the use of the optimal POVM proposed by Sanders and Milburn [49]. We now consider this state in the context of the present work. Formally, the optimal state is [30]:

$$|\psi\rangle_{\rm opt} = \sum_{\mu=-j}^{j} {\rm C}_\mu |j,\mu\rangle \,, \tag{2.21}$$

where the amplitude is given by

$${\rm C}_\mu = \frac{1}{\sqrt{j+1}} \sin\left[\frac{(\mu+j+1)\pi}{2j+2}\right].$$

It is worth noting that the optimal state is a state *within* the interferometer just like the case of the NOON state. So we use the operator $\hat{Q}$ as the detection operator. It would be a simple beam splitter transformation to obtain the actual MZI input state and this result is given in Ref. [30]. First, we need to transform this state through the phase shifter: $|\psi\rangle_{\varphi|\rm opt} = \sum_{\mu=-j}^{j} e^{-i\mu\varphi} {\rm C}_\mu |j,\mu\rangle$. Then, using Eq. (2.5) we obtain,

$$\langle \hat{Q} \rangle_{\varphi|\rm opt} = \sum_{\nu=-j}^{j} (-1)^{2\nu} {\rm C}_{-\nu} {\rm C}_\nu e^{i2\nu\varphi}. \tag{2.22}$$

Plugging the above equation into Eq. (2.4) we can calculate $\delta\varphi$. However, we have not found a closed form expression for $\delta\varphi$. Instead, Fig. 2.4(b) shows a numerical plot. Clearly the optimal state gives a sub-shot noise level and does better for large photon number.

TABLE 2.1. Phase estimate for various input states under parity detection. Here, Row 1: Coherent state at one input ($\hat{a}_{in}$). Row 2: Number state at one input ($\hat{a}_{in}$). Row 3: Dual Fock state. Row 4: Yurke state. Row 5: Modified Yuen state. Row 6: State suggested by Smerzi and Pezzi. The states in 7 and 8 are states representing the modes $\hat{a}'$ and $\hat{b}'$ *within* the interferometer. In the Schwinger notation, $\hat{J}_y$ eigen states represent the internal modes $\hat{a}'$ and $\hat{b}'$(see Ref. [51]). Row 7: Optimal state. Row 8: NOON state.

	Input State		Phase Estimate
	Fock- state Notation	Schwinger Notation	$\delta\phi$
1.	$\left\|\alpha\right\rangle_a \left\|0\right\rangle_b$	$\sum_{2j=0}^{\infty} e^{-\frac{\|\alpha\|^2}{2}} \frac{(\alpha)^{2j}}{\sqrt{(2j)!}} \left\|j,j\right\rangle$	$\frac{1}{\sqrt{N}}$(SL)
2.	$\left\|N\right\rangle_a \left\|0\right\rangle_b$	$\sum_{\mu=-j}^{j} \delta_{\mu,j} \left\|j,j\right\rangle$	$\rightarrow \frac{1}{\sqrt{N}}$
3	$\left\|N\right\rangle_a \left\|N\right\rangle_b$	$\sum_{\mu=-j}^{j} \delta_{\mu,0} \left\|j\mu\right\rangle$	$\frac{\sqrt{2}}{\sqrt{N(N+2)}} \approx \frac{\sqrt{2}}{N}$
4.	$\frac{1}{\sqrt{2}}\left[\left\|\frac{N}{2}\right\rangle_a \left\|\frac{N}{2}\right\rangle_b + \left\|\frac{N}{2}+1\right\rangle_a \left\|\frac{N}{2}-1\right\rangle_b\right]$	$\sum_{\mu=-j}^{j} \frac{(\delta_{\mu,0}+\delta_{\mu,1})}{\sqrt{2}} \left\|j,\mu\right\rangle$	$\rightarrow \frac{1}{\sqrt{\frac{N}{2}(\frac{N}{2}+1)}} \approx \frac{\sqrt{2}}{N}$
5.	$\frac{1}{\sqrt{2}}\left[\left\|\frac{N+1}{2}\right\rangle_a \left\|\frac{N-1}{2}\right\rangle_b + \left\|\frac{N-1}{2}\right\rangle_a \left\|\frac{N+1}{2}\right\rangle_b\right]$	$\sum_{\mu=-j}^{j} \frac{(\delta_{\mu,1/2}+\delta_{\mu,-1/2})}{\sqrt{2}} \left\|j,\mu\right\rangle$	sub-shot noise [Fig. 2.4(a)]
6.	$\frac{1}{\sqrt{2}}\left[\left\|\frac{N}{2}+1\right\rangle_a \left\|\frac{N}{2}-1\right\rangle_b + \left\|\frac{N}{2}-1\right\rangle_a \left\|\frac{N}{2}+1\right\rangle_b\right]$	$\sum_{\mu=-j}^{j} \frac{(\delta_{\mu,1}+\delta_{\mu,-1})}{\sqrt{2}} \left\|j,\mu\right\rangle$	sub-shot noise [Fig. 2.4(b)]
7.	$\sqrt{\frac{2}{N+1}} \sum_{k=0}^{N} \sin\left[\frac{(N+2+k)\pi}{2(N+2)}\right] \left\|\frac{N+k}{2}\right\rangle_{a'} \left\|\frac{N+k}{2}\right\rangle_{b'}$	$\sum_{\mu=-j}^{j} \frac{\sin(\frac{(\mu+j+1)\pi}{2j+2})}{\sqrt{j+1}} \left\|j,\mu\right\rangle_y$	sub-shot noise [Fig. 2.4(c)]
8.	$\frac{1}{\sqrt{2}}\left\|N\right\rangle_{a'} \left\|0\right\rangle_{b'} + \left\|0\right\rangle_{a'} \left\|N\right\rangle_{b'}$	$\sum_{\mu=-j}^{j} \frac{(\delta_{\mu,j}+\delta_{\mu,-j})}{\sqrt{2}} \left\|j,\mu\right\rangle_y$	$\frac{1}{N}$ (HL)

It is worth noting that, although one can generate the optimal state, the implementation of the optimal POVM [30] for which $|\psi\rangle_{\rm opt}$ is designed for, requires a real time feedback. The variance in this case is [30]:

$$\delta\varphi_{opt} = \tan\left(\frac{\pi}{N+2}\right) \approx \frac{\pi}{N}. \tag{2.23}$$

The parity detection, on the contrary, is relatively straightforward. The variance thus obtained due to optimal POVM and parity detection for the $|\psi\rangle_{\rm opt}$ is shown in Fig. 2.4(b).

Finally we consider the input state, recently suggested by Smerzi and Pezzi [52] for achieving the HL, given by

$$|\psi\rangle_{\rm sp} = \frac{(|j,1\rangle + |j,-1\rangle)}{\sqrt{2}}. \tag{2.24}$$

The strategy employed by these authors is direct detection of number of photons at the output modes of MZI and applying Bayesian analysis for multiple detections with greater confidence. Also it is important to note that Eq. (2.4) was not used to calculate the variance but a single interferometric measurement was used. In this sense, it is claimed [52] that the above state is the most optimal one for the HL. Such a quantum state of Eq. (2.24) was also considered in Ref [28] with the $\hat{J}_z$ measurement.

Here we apply parity detection to the input state $|\psi\rangle_{\rm sp}$. Using Eq. (2.10), we immediately get the following result:

$$\langle\hat{P}\rangle_{\rm sp} = (-1)^{j+1}(d^j_{1,1}(2\varphi) + d^j_{-1,1}(2\varphi)), \tag{2.25}$$

and the phase variance can be calculated using Eq. (2.4). We plot the result numerically Fig. 2.4(b), in the limit of $\varphi \to 0$. And we clearly see the sub-shot noise limit. Indeed for the large number of input photons, the phase estimate approaches the HL.

2.4 Conclusions

In this chapter, we demonstrate the importance of the parity detection scheme in the optical phase estimation. By considering the combination of a NOON state and a dual-

Fock state at the input, we have shown that the parity detection still gives sub-shot noise variance, and it reaches close to the HL for large input number of photons. We have also considered the Yuen state, the so-called optimal state, and the state suggested by Smerzi and Pezze, and have shown that we can achieve even smaller phase variance using the parity detection. Our results indicate that the parity detection acts as a unified detection scheme for precision phase measurements. We have summarized the results in the Table 2.1.

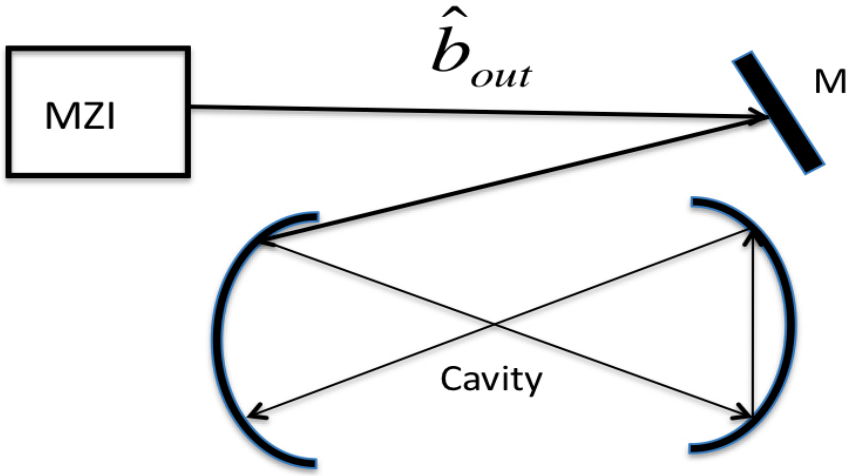

FIGURE 2.5. Schematic of containing the detecting output mode $\hat{b}_{out}$ from the MZI in Fig. 2.1 in a cavity towards measuring the parity of the mode as suggested in Ref. [72]. The output mode is reflected at mirror, M, and then fed into the cavity. By properly picking the curvature of the cavity morrors, one can trap the mode for sufficiently long time.

From a mathematical point of view, the parity detection appears to be simple in comparison to any other strategy, but to experimentally realize such a detection scheme is not trivial. There are basically two different approaches to accomplish the task in laboratory. The simplest one is by employing number-resolving photodetectors [70, 73, 74, 75, 76, 77, 78] at the output detecting mode (mode $\hat{b}_{out}$ in Fig. 4.4). It should be noted that we not necessarily need a photodetector at single photon resolution, instead we need a detector that would discriminate even and odd number of photons.

Alternatively one can measure the wigner function. In Ref. [79] it has been shown that expectation value of the parity is $h/2$ times the wigner function. In Ref. [72], it has been shown that if we can store the single mode field in a cavity then one can perform the parity detection by measuring the wigner function. This would require containing the output detecting mode $\hat{b}_{out}$ in a cavity as shown in Fig. 2.5. By properly picking the curvature of the cavity morrors, one can trap the mode for sufficiently long time. This approach is discussed further in Ref. [80].

3 Canonical Phase Measurement in the Presence of Photon Loss

3.1 Introduction

Canonical phase measurement in quantum mechanics is a significant problem, for the main reason that phase is a quantity that is conjugate to the number, N, of photons in a particular electromagnetic mode [48, 81, 82]. Due to this conjugate nature, the phase estimate $\Delta\varphi$ is ultimately limited by the number N of the photons as $\Delta\varphi = 1/N$, which is conventionally referred as the Heisenberg limit. In the usual classical setting, such as interferometry with lasers, for a given number of input resources, N, phase estimate scales as $1/\sqrt{N}$, which is usually referred as shot-noise limit.

Accurate phase estimation has many practical applications such as metrology, imaging and sensing [83]. Achieving Heisenberg limit in practice is not a trivial problem and there have been numerous proposals to achieve this limit [3, 4, 51, 30, 70, 57, 27, 26, 37, 28, 36]. Canonical phase measurement has been first dealt with Helstrom [84] and Shapiro [85], and later Sanders and Milburn [86, 87] used it to obtain a phase estimate in a Mach-Zehender interferometer (MZI) as shown in Fig.3.1 (excluding the loss part). The phase estimate thus obtained is independent of the system phase, unlike in other methods [4, 51, 70] where the ultimate limit is achieved for a particular system phase. Also, the measurement specified by Sanders and Milburn is not particular to a specific input state.

Motivated by this work, Berry and Wiseman [30] analytically derived an input state, called as the optimal state, subject to the canonical measurement. They also suggested an adaptive method of approximately implementing the canonical phase measurement [30, 31], which has been used in the recent experimental realization of the Heisenberg limited phase measurement by Higgins *et al.* [66]. The canonical measurement, written as a

Positive Operator Valued Measure(POVM) by Sanders and Milburn [86] is,

$$\hat{F}(\varphi)d\varphi = \frac{2j+1}{2\pi} \left|j\varphi\right\rangle \left\langle j\varphi\right| d\varphi, \tag{3.1}$$

in terms of the phase states

$$\left|j\varphi\right\rangle = \frac{1}{\sqrt{2j+1}} \sum_{\alpha=-j}^{j} e^{i\alpha\varphi} \left|j\alpha\right\rangle_y .$$

In defining this, the Schwinger's representation is used, and for completeness we wish to outline the notation. The three angular momentum components $\hat{J}_x, \hat{J}_y$ and $\hat{J}_z$ are very effective in analyzing two-port, lossless, interferometers [4, 86, 51]. For the two modes, $\hat{a}$ and $\hat{b}$ of the MZI (Fig. 3.1), these two mode operators are,

$$\hat{J}_x = (\hat{a}^\dagger \hat{b} + \hat{a}\hat{b}^\dagger)/2, \qquad \hat{J}_y = (\hat{a}^\dagger \hat{b} - \hat{a}\hat{b}^\dagger)/2i,$$
$$\hat{J}_z = (\hat{a}^\dagger \hat{a} - \hat{b}^\dagger \hat{b})/2, \qquad \hat{J}^2 = \hat{J}_x^2 + \hat{J}_y^2 + \hat{J}_z^2.$$

In the context of the MZI, $\hat{J}_x$ implements the operation of a 50-50 beam splitter as $e^{i(\pi/2)\hat{J}_x}$ and $\hat{J}_z$ defines the photon number difference in two modes. The simultaneous eigenvector of $\hat{J}^2$ and $\hat{J}_z$, $\left|j,m\right\rangle_z$ represents the joint input state $\left|j+m\right\rangle_{a_{in}}$ and $\left|j-m\right\rangle_{b_{in}}$ in the Fock-state basis, and the total input number of photons is $N = 2j$. The simultaneous eigenvector of $\hat{J}^2$ and $\hat{J}_y$, which is $\left|j,n\right\rangle_y$, represents the joint state *within* the interferometer. The beamsplitter transformation in this representation performs a rotation about the $\hat{J}_x$. The phase states discussed above, are defined in terms of states *within* the interferometer in Fig. 3.1 and thus the output modes or detectors are irrelevant for the present purpose. Thus the probability distribution for the system phase ϕ is obtained as

$$P(\varphi)d\varphi = \left\langle\psi\right| \hat{F}(\varphi) \left|\psi\right\rangle d\varphi = \mathrm{Tr}[\rho\hat{F}(\varphi)]d\varphi. \tag{3.2}$$

Note that φ is the estimate of the system phase ϕ. The optimal state, to be specified below, is derived conditioned upon minimizing the Holevo variance calculated from the

above probability distribution. The Holevo phase variance is defined as [88]

$$(\Delta\varphi)^2 \equiv -1 + |\langle e^{i\varphi}\rangle|^{-2}, \tag{3.3}$$

where $|\langle e^{i\varphi}\rangle| = \int_0^{2\pi} d\varphi P(\varphi) e^{i\varphi-\bar{\varphi}}$, is also called the sharpness. Here $\bar{\varphi}$ is a mean phase and we take it to be zero. The Holevo variance for the optimal state is given by Ref. [30, 31],

$$(\Delta\varphi)^2 = \tan^2(\frac{\pi}{N+2}) \approx \frac{\pi^2}{N^2}, \tag{3.4}$$

thus giving rise to a phase estimate that scales as the Heisenberg limit. Besides the

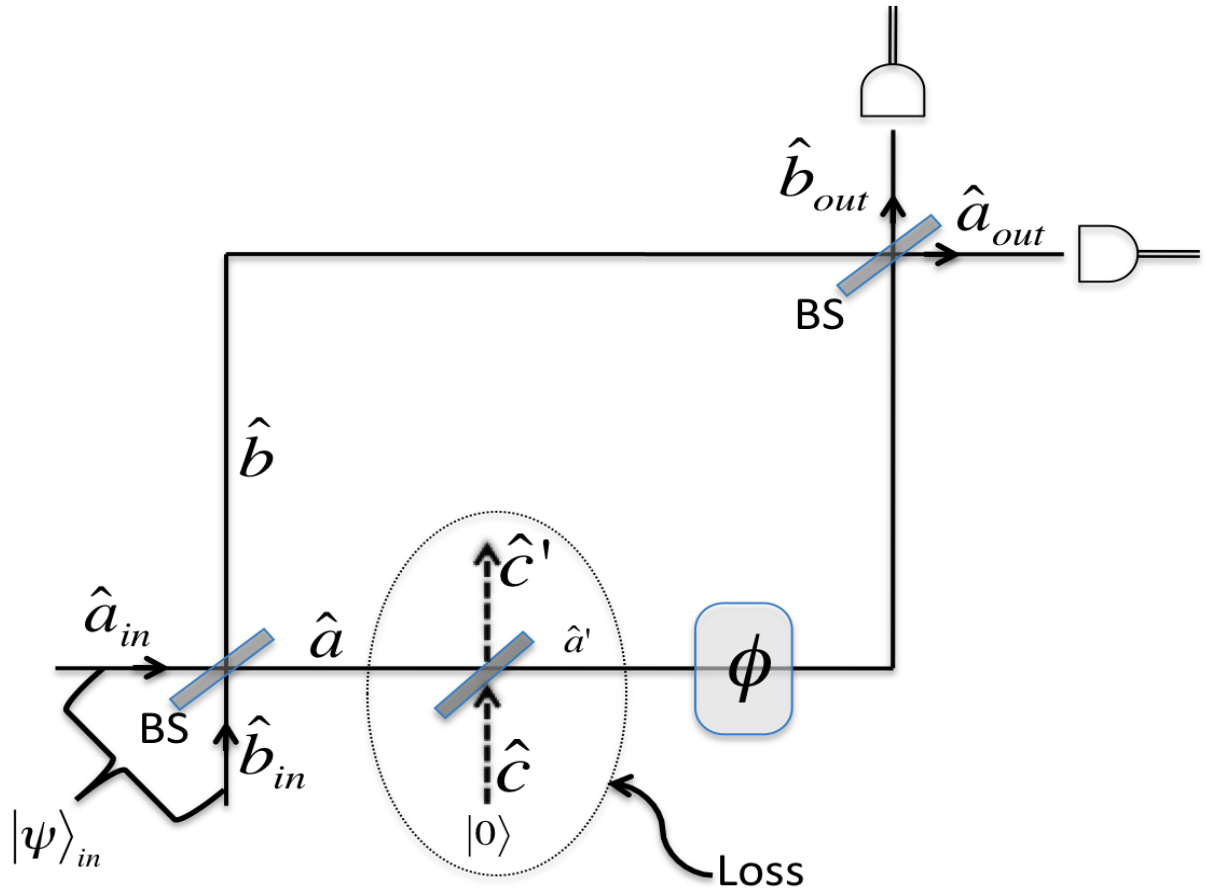

FIGURE 3.1. Schematic of Mach-Zehender Interferometer (MZI) with photon loss at the phase shift. The state $|\psi\rangle_{\text{in}}$ represents the joint input state at $\hat{a}_{\text{in}}$ and $\hat{b}_{\text{in}}$. Photons in the lower arm first encounter the fictitious beam splitter (BS), for which vacuum enters through the other input, and depending the transmission coefficient, some of them are scattered into the mode $\hat{c}'$, which are ignored (traced out), and the remaining pass through the phase shifter.

optimal state, other prominent states that achieve the Heisenberg limit are so called the

NOON states [4, 37] and the dual-fock state [70, 57]. Formally the NOON state is,

$$|\psi\rangle_N = \frac{|N\rangle_{\hat{a}}\,|0\rangle_{\hat{b}} + |0\rangle_{\hat{a}}\,|N\rangle_{\hat{b}}}{\sqrt{2}}. \tag{3.5}$$

Note that the above state is not an input state at the MZI shown in Fig.1, but a state *within* the interferometer and the subscripts $\hat{a}$ and $\hat{b}$ denotes the internal modes of the MZI. The dual-fock input state is given as,

$$|\psi\rangle_D = |N\rangle_{\hat{a}_{in}}\,|N\rangle_{\hat{b}_{in}} \tag{3.6}$$

The detection scheme for both, the NOON and the dual-fock state that results in the Heisenberg limited phase estimate is the parity detection [57, 69], first proposed by Bollinger *et al.* [37] in the context of frequency metrology with trapped ions. The shot-noise and sub shot-noise limit with matter wave interferometry which deals with Bose-Einstein condensates at the input of the MZI is studied in Refs. [52].

It is natural to question the performance of such states or the detection schemes in a more realistic conditions such as photon loss associated with the propagation. The analysis of the NOON states under propagation loss was carried out independently by Gilbert *et al.* [33] and by Rubin and Kaushik [32], where they used pure state formalism. In Ref. [33, 32] for NOON state, the minimum number of photons required to achieve a minimum detectable phase in presence of loss is also given.

In this chapter we study the performance of optimal state and the optimal POVM in the presence of the photon loss associated with propagation. We use the generic beam splitter model for photon loss [89], as shown in Fig. 3.1. The input mode $\hat{c}$ for this fictitious beam splitter is a vacuum mode, and the output mode $\hat{c}'$ is then to be traced out. This typically implies that the photons that are lost in mode $\hat{c}'$, due to the nonzero reflection coefficient r, correspond to the photon loss.

In the following two Sections we describe optimal state in presence of photon loss and carry out the explicit density matrix calculation. In Section 4.4, we quantitatively describe

the effect of photon loss on the canonical phase estimation. Section 3.5 concludes with numerical results and discussions.

3.2 Optimal State in Presence of Photon Loss

We now proceed to develop the mathematical framework to study optimal-state canonical interferometry with photon loss. The beam splitter representing loss, with arbitrary transmission and reflection, can be characterized by an angle θ, such that transmission and reflection coefficients are $\tau = \cos^2(\theta/2)$ and $r = 1-\cos^2(\theta/2)$, respectively. Therefore, the loss is simply the reflection coefficient,

$$L = r = 1 - \cos^2(\theta/2). \tag{3.7}$$

The action of such an arbitrary beam splitter on an arbitrary joint input state $|j, a\rangle$ in Schwinger notation, is simply given as [51],

$$e^{i\theta \hat{J}_x} |j, a\rangle = \sum_{b=-j}^{j} e^{i\theta(b-a)} d^j_{a,b}(\theta) |j, b\rangle , \tag{3.8}$$

where $d^j_{a,b}(\theta)$ is the usual rotational matrix element given as:

$$d^j_{a,b}(\theta) = (-1)^{a-b} 2^{-a} \sqrt{\frac{(j-a)!(j+a)!}{j-b)!(j+b)!}} P^{(a-b,a+b)}_{j-a}(\cos\theta)(1-\cos\theta)^{\frac{a-b}{2}}(1+\cos\theta)^{\frac{a+b}{2}}, \tag{3.9}$$

where $P^{(\alpha,\beta)}_n(x)$ is the Jacobi polynomial [68]. Also it is worth noting that when converted to Fock-basis, a two mode joint state in Schwinger notation, $|j, a\rangle$ is $|j+a\rangle\,|j-a\rangle$.

The optimal state was originally derived by Berry and Wiseman [30] conditioned on minimizing the phase variance with the canonical probability distribution given in Eq. (3.2). Formally the optimal state is,

$$|\psi\rangle_{\text{opt}} = \sum_{\mu=-j}^{j} \frac{1}{\sqrt{j+1}} \sin\left[\frac{(\mu+j+1)\pi}{2j+2}\right] |j\mu\rangle_y . \tag{3.10}$$

Recall that the simultaneous eigenstate of $\hat{J}^2$ and $\hat{J}_y$ denote the state *within* the interferometer, and thus the above state is after the first beam splitter, while $|j+\mu\rangle_a$ and

$|j-\mu\rangle_b$ represents the fock state corresponding to modes $\hat{a}$ and $\hat{b}$ respectively. Rewriting the above state in a more explicit form as the product of the states at the two arms of the interferometer as,

$$|\psi\rangle_{\text{opt}} = \sum_{\mu=-j}^{j} \psi_\mu \, |j+\mu\rangle_a \, |j-\mu\rangle_b \,, \tag{3.11}$$

where

$$\psi_\mu = \frac{1}{\sqrt{j+1}} \sin\left[\frac{(\mu+j+1)\pi}{2j+2}\right].$$

With the loss in mode $\hat{a}$, which is represented by the fictitious beam splitter, and $|0\rangle_c$ is the state entering the other input port, the combined input state for the fictitious beam splitter is: $|j+\mu\rangle_a \, |0\rangle_c$, and thus the state to be considered is,

$$|\psi\rangle = |\psi\rangle_{\text{opt}} \otimes |0\rangle_c = \sum_{\mu=-j}^{j} \psi_\mu \, |j+\mu\rangle_a \, |j-\mu\rangle_b \, |0\rangle_c \,. \tag{3.12}$$

The fictitious beam-splitter transforms modes $\hat{a}$ and $\hat{c}$ to modes $\hat{a}'$ and $\hat{c}'$ respectively. Making use of the Schwinger representation for modes $\hat{a}$ and $\hat{c}$, the input $|j+\mu\rangle_a \, |0\rangle_c$ for the fictitious beam splitter can be written as a joint state: $\left|\frac{j+\mu}{2}, \frac{j+\mu}{2}\right\rangle_{a,c}$. Letting $k = (j+\mu)/2$ and using Eq. (3.8) we have the output as,

$$\begin{aligned} e^{i\theta \hat{J}_x} \, |k,k\rangle_{a,c} &= \sum_{m=-k}^{k} e^{i\frac{\pi}{2}(m-k)} d^k_{mk}(\theta) \, |k,m\rangle_{a'c'} \\ &= \sum_{m=-k}^{k} e^{i\frac{\pi}{2}(m-k)} d^k_{mk}(\theta) \, |k+m\rangle_{a'} \, |k-m\rangle_{c'} \,. \end{aligned} \tag{3.13}$$

Therefore the pure state of the inner modes $\hat{a}'$, $\hat{b}$ of the interferometer, and mode $\hat{c}'$ of the lost photons is given as,

$$|\psi\rangle = \sum_{\mu=-j}^{j} \sum_{m=-k}^{k} \psi_\mu e^{i\frac{\pi}{2}(m-k)} d^k_{mk}(\theta) \, |k+m\rangle_{a'} \, |k-m\rangle_{c'} \, |j-\mu\rangle_b \,, \tag{3.14}$$

where $k = (j+\mu)/2$ and $d^k_{mk}(\theta)$ is the usual rotational matrix element, as defined earlier.

3.3 Density Matrix Description

The state specified in Eq. (3.14) is a pure state and cannot be used further, so we need to calculate the reduced density matrix, by tracing out, mode $\hat{c}'$, as we have no more access to the lost photons. Thus first we need to calculate the total density matrix, representing the pure state of Eq. (3.14),

$$\rho = |\psi\rangle \langle\psi| , \tag{3.15}$$

which upon invoking $|\psi\rangle$ from Eq. 3.14 results in

$$\begin{aligned}\rho = \sum_{\mu,\nu=-j}^{j} \sum_{m=-k}^{k} \sum_{n=-k'}^{k'} \psi_\mu \psi_\nu d^k_{m,k}(\theta) d^{k'}_{n,k'}(\theta) e^{i\frac{\pi}{2}(m-k)} e^{-i\frac{\pi}{2}(n-k')} \\ \times |k+m\rangle_{a'} |k-m\rangle_{c'} |j-\mu\rangle_{b\ a'} \langle k'+n|_{c'} \langle k'-n|_b \langle j-\nu| ,\end{aligned} \tag{3.16}$$

where $k' = (j+\nu)/2$. The total density matrix given in Eq. (3.16) explicitly represents the state within the interferometer for a given loss, characterized by the angle θ, and is useful in analyzing lossy interferometers such as the present one.

As the mode $\hat{c}'$ is to be ignored, we need the reduced density matrix by tracing out that mode from the total density matrix given in Eq. (3.16). Thus we have,

$$\begin{aligned}\rho' = \mathrm{Tr}_{c'}[|\psi\rangle \langle\psi|] = \sum_{\mu,\nu=-j}^{j} \sum_{m=-k}^{k} \sum_{n=-k'}^{k'} \psi_\mu \psi_\nu d^k_{m,k}(\theta) d^{k'}_{n,k'}(\theta)) e^{i\frac{\pi}{2}(m-k)} e^{-i\frac{\pi}{2}(n-k')} \\ \times |k+m\rangle_{a'} |j-\mu\rangle_{b\ a'} \langle k'-n|_b \langle j-\nu| \, [{}_{c'}\langle k-m|k'-n\rangle_{c'}] .\end{aligned} \tag{3.17}$$

Noting that ${}_{c'}\langle k-m|k'-n\rangle_{c'} = \delta_{k-m,k'-n}$, which eliminates the two exponential terms in Eq. (3.17). This leads to:

$$\rho' = \sum_{\mu,\nu=-j}^{j} \sum_{m=-k}^{k} \sum_{n=-k'}^{k'} \psi_\mu \psi_\nu d^k_{m,k}(\theta) d^{k'}_{n,k'}(\theta) \delta_{k-m,k'-n} |k+m\rangle_{a'} |j-\mu\rangle_{b\ a'} \langle k'-n|_b \langle j-\nu| .$$

We can now use Eq. (3.18) in Eq. (3.2) to obtain the probability distribution and thus the minimum detectable phase as a function of θ-which characterizes the photon loss-and the input photon number $2j$.

3.4 Phase Estimate in Presence of Photon Loss

To get an estimate using Holevo phase variance, we need to calculate the probability distribution, $P(\varphi)$ using Eq.(3.2). But in presence of the loss, few of the input photons are not accessible by the POVM. In cases like this the probability distribution is given as (see Ref. [90, 84]),

$$P(\varphi) = \frac{\mathrm{Tr}[\rho' \hat{F}(\varphi)]}{\int_0^{2\pi} \mathrm{Tr}[\rho' \hat{F}(\varphi)] d\varphi} \tag{3.19}$$

Note that φ is an estimate of the system phase ϕ.

The POVM, $\hat{F}(\varphi)d\varphi$ [Eq. (3.1)] is given in terms of the $\hat{J}_y$ eigen states. Noting that the $\hat{J}_y$ eigen states are the states of the modes *within* the interferometer, we can rewrite the POVM as,

$$\hat{F}(\varphi) = \frac{1}{2\pi} \sum_{\alpha,\beta=-j}^{j} e^{i(\alpha-\beta)\varphi} \left|j, \alpha\right\rangle_y \left\langle j, \beta\right| . \tag{3.20}$$

Since the joint state $\left|j, \alpha\right\rangle_y$ is written as $\left|j+\alpha\right\rangle_{a'} \left|j-\beta\right\rangle_b$, we have,

$$\hat{F}(\varphi) = \frac{1}{2\pi} \sum_{\alpha,\beta=-j}^{j} e^{i(\alpha-\beta)\varphi} \left|j+\alpha\right\rangle_{a'} \left|j-\alpha\right\rangle_b \otimes_{a'} \left\langle j+\beta\right|_b \left\langle j-\beta\right| \tag{3.21}$$

After the fictitious beamsplitter which represents photon loss associated with propagation, the inner modes of the MZI are $\hat{a}'$ and $\hat{b}$, and so the $\hat{J}_y$ eigen states are the product states of these modes. Thus using Eq. (3.21) along with Eq. (3.18) for the reduced density matrix, after carrying out the trace operation for the modes $\hat{a}'$ and $\hat{b}$, we have in presence of loss,

$$\begin{aligned}\mathrm{Tr}[\rho' \hat{F}(\varphi)] = \frac{1}{2\pi} \sum_{\substack{\mu,\nu=-j \\ \alpha,\beta=-j}}^{j} \sum_{m=-k}^{k} \sum_{n=-k'}^{k'} [\psi_\mu \psi_\nu d^k_{m,k}(\theta) d^{k'}_{n,k'}(\theta) \\ \times e^{i(\alpha-\beta)\varphi} \langle k'-n|j+\alpha\rangle \langle j+\beta|k+m\rangle \\ \times \langle j-\beta|j-\mu\rangle \langle j-\nu|j-\alpha\rangle]\end{aligned} \tag{3.22}$$

Recalling $k' = (j+\nu)/2$, $k = (j+\mu)/2$, and because $\beta = \mu$ and $\alpha = \nu$ as a consequence of the last two inner products in the above equation, we get from the first two inner products $n = k'$ and $m = k$ respectively. Hence

$$\mathrm{Tr}[\rho'\hat{F}(\varphi)] = \frac{1}{2\pi}\sum_{\mu,\nu=-j}^{j}\psi_\mu\psi_\nu e^{i(\nu-\mu)\varphi}d^k_{k,k}(\theta)d^{k'}_{k',k'}(\theta) \tag{3.23}$$

and

$$\int_0^{2\pi}\mathrm{Tr}[\rho'\hat{F}(\varphi)]d\varphi = \sum_{\mu,\nu=-j}^{j}\psi_\mu\psi_\nu\delta_{\nu,\mu}d^k_{k,k}(\theta)d^{k'}_{k',k'}(\theta). \tag{3.24}$$

From the definitions of k andk' we see that $k = k'$ when $\mu = \nu$. Therefore using the rotational matrix element in Eq. (3.9), we have $d^k_{k,k}(\theta)d^{k'}_{k',k'}(\theta) = \left[\cos^2\frac{\theta}{2}\right]^{(k+k')} = (1-L)^{2k}$. Using this in Eq. (3.19) we get the probability distribution as,

$$P(\varphi) = \frac{\sum_{\mu,\nu=-j}^{j}\psi_\mu\psi_\nu e^{i(\nu-\mu)\varphi}d^k_{k,k}(\theta)d^{k'}_{k',k'}(\theta)}{2\pi\sum_{\mu=-j}^{j}|\psi_\mu|^2(1-L)^{(j+\mu)}} \tag{3.25}$$

With this probability distribution we can calculate any moments of the phase estimate as a function of loss, θ. Here we calculate the Holevo phase variance rather than the standard variance, because the optimal state is derived by minimizing the Holevo phase variance [30]. Using Eq. (3.25) we now calculate sharpness $|\langle e^{i\varphi}\rangle|$ is given as,

$$\begin{aligned}|\langle e^{i\varphi}\rangle| &= \int_0^{2\pi}P(\varphi)e^{i\varphi}d\varphi \\ &= \frac{\sum_{\mu,\nu=-j}^{j}\delta_{\nu,\mu-1}\psi_\mu\psi_\nu d^k_{k,k}(\theta)d^{k'}_{k',k'}(\theta)}{\sum_{\mu=-j}^{j}|\psi_\mu|^2(1-L)^{(j+\mu)}},\end{aligned} \tag{3.26}$$

where $\delta_{\nu,\mu-1} = \frac{1}{2\pi}\int_0^{2\pi}e^{(\nu-\mu+1)\varphi}d\varphi$ and invoking the definition of k and k' in Eq. (3.26), we obtain

$$|\langle e^{i\varphi}\rangle| = \frac{\sum_{\mu=-j}^{j}\psi_\mu\psi_{\mu-1}(1-L)^{j+\mu-\frac{1}{2}}}{\sum_{\mu=-j}^{j}|\psi_\mu|^2(1-L)^{(j+\mu)}}, \tag{3.27}$$

for the expression of the so-called sharpness as a function of loss. We use Eq. (3.27) in Eq. (3.3) to obtain the phase estimate as a function of loss.

3.5 Conclusions

Now the minimum detectable phase shift can be found with the uncertainty in phase estimate by plugging Eq. (3.27) in Eq. (3.3). In Fig. 3.2 we numerically plot the minimum

detectable phase $\Delta\varphi$ as a function of $2j = N$, the number of input photons, for three different values of loss, $L = 10\%$ and $L = 30\%$ and $L = 85\%$. For comparison we also plot the Heisenberg limit for the optimal state given in Eq. (3.4). Interestingly, the optimal POVM results in a phase estimate in presence of loss that does not diverge unlike the results of NOON states presented in Ref. [33, 32].

As we do not have a closed form expression for the Holevo variance, as a function of loss L and input photon number N, we have not found an analytical form for what exact amount of loss does the estimate exceed the shot-noise limit. So we numerically plot in Fig. 3.2. We see that up to a loss of 30% we will be able to get a sub-shot noise limit.

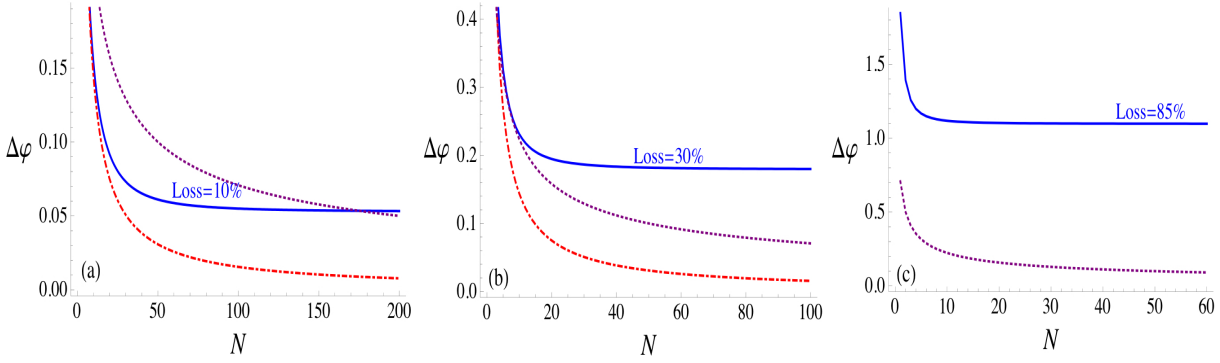

FIGURE 3.2. Plot of minimum detectable phase versus the input photon number $N = 2j$ for two different values of loss. (a) $L = 0.1$, (b) $L = 0.3$ and (c)$L = 0.85$. The dotted line in both figures is the shot noise limit $1/\sqrt{2j}$ and the dashed line in (a) is the Heisenberg limit given be Eq. (3.4), for comparison.The solid lines are numerically evaluated using Eq. (3.3) and Eq. (3.27).

From a practical considerations this result is significant for two reasons. First, even for loss of about 25% of the photons in the mode passing through the phase shift, we still can have sub-shot noise limited phase estimate albeit we need to operate the interferometer with appropriate input photon number as indicated in Fig. 3.2(b). Second, the estimate does not blow up for any amount of loss. This means if we begin with large number of input photons in optimal state, we still get a sensible value for phase estimate.

To summarize, we analyzed the canonical phase measurement in presence of photon loss. Our formalism is based on the density matrix, which describes the mixed states,

which naturally arise due to the presence of loss. Our analysis shows that the minimum detectable phase is not monotonically decreasing function and would tend to saturate at certain photon numbers, depending the loss present. Nevertheless, we can for small loss have considerably high number of input photons for the optimal state, that achieve sub-shot noise level phase estimates.

4 Rapid-purification Protocols for Optical Homodyning

4.1 Introduction

In this chapter, we shall deal with extracting information while continually measuring a two level quantum system. The contents of this chapter are published in Physical Review A **77**, 012102 (2008). Reprinted with the permission of the American Physical Society, as stated in the FAQ section for authors and is provided in the Appendix.

Using feedback one can actually increase the rate at which we draw information from the system. Quantum feedback control is the domain of quantum measurements where the system is driven to a specific target state by modifying the measurement dynamics as the measurement progresses [91, 92]. The field of quantum feedback was introduced by by Wiseman and Milburn [93], where they considered instantaneous feedback of some measured photo current onto the dynamics of the system. The general schematic is shown in Fig. 4.1.

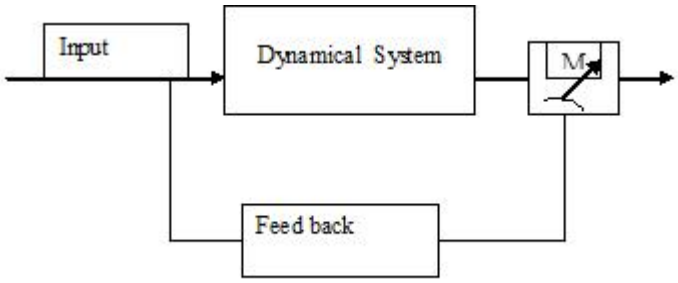

FIGURE 4.1. Schmatic of Feedback scheme. The dynamical system corresponds to external perturbations such as dissipations and other perturbations arising due to the interaction of the system with the environment. The measurement is indicated in a separate box as we wish to have complete control on measurement.

Rapid-purification protocols increase the rate at which the state of a system is purified by a continuous measurement [94, 95, 96, 97, 98, 99, 100, 101, 102]. They do this by

applying feedback control to the system as the measurement proceeds. All such protocols described to date have been devised for continuous measurements of an observable (that is, measurements that are not dissipative). Under this kind of measurement the evolution of the system density matrix, ρ, is given by the stochastic master equation [92, 103, 104],

$$d\rho \;=\; -(i/\hbar)[H,\rho]dt - k[X,[X,\rho]]dt + \sqrt{2k}(X\rho + \rho X - 2\langle X\rangle\rho)dW, \qquad (4.1)$$

where X is the hermitian operator corresponding to the observable being measured, H is the Hamiltonian of the system, dW is Gaussian white noise satisfying the Ito calculus relation $dW^2 = dt$. The observers continuous measurement record, which we will denote by $r(t)$, is given by $dr = \langle X\rangle dt + dW/\sqrt{8k}$. This kind of measurement will project the system onto an eigenstate of X after a time $t \gg 1/(\Delta^2 k)$, where Δ is the difference between the two eigenvalues of X that are nearest each other.

Photon counting and optical homodyning do not fall into the above class of measurements because they subject the system to dissipation. Thus if one has a single optical qubit, consisting of a single mode containing no more than one photon as shown in Fig. 4.2, and one measures it with a photon counter, then regardless of whether the measurement tells us that the state was initially $|0\rangle$ or $|1\rangle$, as $t \to \infty$ the final state is always $|0\rangle$. If we wish we can think of this as a measurement of the photon number (that is, a measurement in the class above with $X = a^\dagger a$), followed by an irreversible operation that takes both $|0\rangle$ and $|1\rangle$ to the vacuum.

The physical system that we consider is a single mode of radiation or simply a single photon in a cavity as shown in the Fig. 4.2. The cavity has a decay rate γ and the leaked photon is subjected to homodyne detection. The feedback is acted by adjusting the local oscillator phase as the measurement progresses.

Our purpose here is to examine whether there exist rapid-purification feedback protocols for homodyne detection performed on a single optical qubit, and if so, to compare

their properties with those pertaining to a continuous measurement of an observable on a single qubit. Our motivation is partly theoretical interest regarding the effect of dissipation on rapid-purificaton protocols, and partly to explore whether such protocols can be implemented in an optical setting. Before we begin it is worth recalling the properties of the single-qubit rapid-purification protocols that have been derived to date for non-dissipative measurements. The first is the protocol introduced by one of us [94] (see also [102]) in which one applies feedback control to speed up the increase in the *average* purity of the system. The average here is taken over all possible realizations of the measurement (all possible measurement records $r(t)$). The protocol involves applying feedback during the measurement to keep the Bloch vector of the state of the qubit perpendicular to the basis of the measured observable, X. In the limit of strong feedback, and high final average purity, this provides a factor of two decrease in the time required to reach a given average purity. In the limit of strong feedback the protocol also eliminates the stochasticity in the purification process, so that the purity increases deterministically.

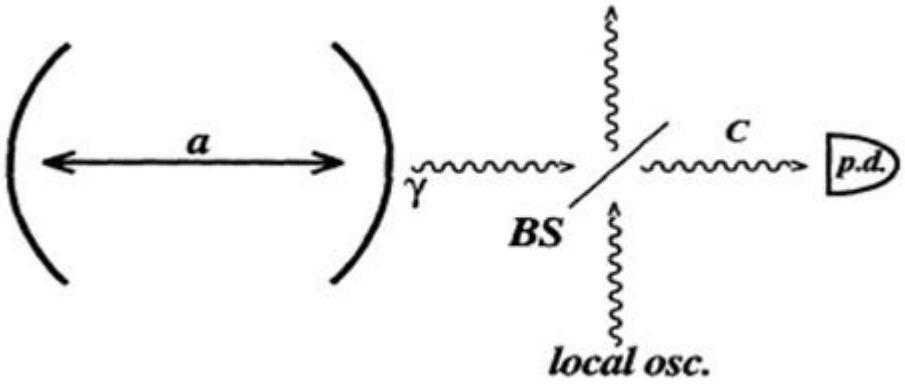

FIGURE 4.2. A single mode of radiation in a cavity with a decay rate of γ. The leaked photon will undergo homodyning where the local oscillator phase and amplitude can be controlled. This would be the case of simple homodyning where beam splitter is assumed to have a transmissivity $\tau \rightarrow 1$.Here P.D is the photo detector.

In the next section we examine homodyne detection of a single optical qubit, and derive a deterministic rapid-purifcation protocol equivalent to the protocol discussed above.

4.2 Rapid Purification for Optical Homodyning

The dynamics of a single mode of an optical cavity, where the output light is monitored via homodyne detection, is given by [105]

$$\begin{aligned} d\rho &= -\gamma D[a]\rho dt + \sqrt{2\eta\gamma}(ae^{i\theta}\rho + \rho a^\dagger e^{-i\theta})dW \\ &\quad -\sqrt{2\gamma}\langle ae^{i\theta} + a^\dagger e^{-i\theta}\rangle\rho dW, \end{aligned} \tag{4.2}$$

where $D[a]\rho \equiv a^\dagger a\rho + \rho a^\dagger a - 2a\rho a^\dagger$, ρ is the state of the mode, a is the mode annihilation operator, γ is the decay rate of the mode from the cavity, and η is the efficiency of the photo detectors. here we have moved into the interaction picture, and thus eliminated the mode Hamiltonian $H_0 = \hbar\omega a^\dagger a$. In this case the observer's measurement record is given by $dr = \langle a + a^\dagger\rangle dt + dW/\sqrt{8\gamma}$. If the state of the mode has no more than one photon, then we can replace a with the Pauli lowering operator $\sigma_- = \sigma_x - i\sigma_y$, and the SME becomes

$$d\rho = -\gamma D[\sigma_-]\rho dt + \sqrt{2\eta\gamma}\left[\sigma_- e^{i\theta}\rho + \rho\sigma_+ e^{-i\theta} - \langle\sigma_x\cos\theta + \sigma_y\sin\theta\rangle\rho\right]dW. \tag{4.3}$$

We now rewrite this equation using the Bloch-sphere representation of the density matrix, $\mathbf{a} = (x, y, z)$, where $\rho = (1/2)(I + \mathbf{a}\cdot\boldsymbol{\sigma})$ and $\boldsymbol{\sigma} = (\sigma_x, \sigma_y, \sigma_z)$ and I is the two-by-two identity matrix. This gives

$$dx = -\gamma x dt + \sqrt{2\eta\gamma}\left[(1+z)\cos\theta - x(x\cos\theta + y\sin\theta)\right]dW, \tag{4.4}$$

$$dy = -\gamma y dt + \sqrt{2\eta\gamma}\left[(1+z)\sin\theta - y(x\cos\theta + y\sin\theta)\right]dW, \tag{4.5}$$

$$dz = -2\gamma(1+z)dt - \sqrt{2\eta\gamma}(1+z)\left[x\cos\theta + y\sin\theta\right]dW. \tag{4.6}$$

Defining the "linear entropy", L, by $L = 1 - \mathrm{Tr}[\rho^2]$, and using the above equations we find that

$$dL = -\gamma\left\{2L[1 - \eta\left(x\cos\theta + y\sin\theta\right)] + (\eta - 1)(1+z)^2\right\}dt + \sqrt{8\eta\gamma}L\left(x\cos\theta + y\sin\theta\right)dW. \tag{4.7}$$

We wish to maximize the rate of decay of L by adjusting the phase of the local oscillator, θ, as the measurement proceeds. Inspection of the above equation makes it clear how to do this: we simply need to choose θ at each time so that $x\cos\theta + y\sin\theta = 0$. This not only maximizes the rate of decay of L, but also eliminates the stochastic terms in dL and dz so that the evolutions of both are deterministic. This parallels the behavior of the rapid-purification algorithm in [94]. When we choose θ at each time to maximize the rate of reduction of L, the evolution of L becomes

$$\frac{dL}{dt} = -\gamma\left[2L + (\eta - 1)(1+z)^2\right]. \tag{4.8}$$

To achieve this we must continually adjust θ so that $\theta(t) = \arg[y(t) - ix(t)]$. With this choice of θ the equation for z is simply $dz/dt = -2\gamma(1+z)$. We now take the initial state to be the maximally mixed single-qubit state $\rho(0) = I/2$. Solving for the evolution of z in this case we have

$$z(t) = e^{-2\gamma t} - 1, \tag{4.9}$$

and the equation of motion for the linear entropy becomes

$$\frac{dL}{dt} = -\gamma\left[2L + (\eta - 1)e^{-4\gamma t}\right]. \tag{4.10}$$

Thus the evolution of the linear entropy, under the rapid-purification feedback algorithm is

$$L_{\mathrm{fb}}(t) = e^{-2\gamma t}\left[\frac{1}{2} + \frac{1}{2}(1-\eta)\left(1 - e^{-2\gamma t}\right)\right]. \tag{4.11}$$

We now need to compare this with the evolution of the average value of the linear entropy in the absence of any feedback. (That is, when θ is fixed during the measurement.) Since we are treating the case when the initial state is maximally mixed, all choices for the fixed value of θ are equivalent, and so we will choose $\theta = 0$ for simplicity. When θ is fixed the evolution of L is stochastic, and thus more complex. Nevertheless, for perfectly efficient detection ($\eta = 1$) the master equation Eq.(4.3) is readily solved by using the linear form of

the equivalent stochastic Schrödinger equation (SSE), being [106] (see also [107, 108, 92]),

$$d|\psi\rangle = \left[-\gamma\sigma_+\sigma_- dt + \sqrt{2\gamma}\sigma_- dW\right]|\psi\rangle \tag{4.12}$$

The solution is

$$\rho(t) = \frac{V(t)\rho(0)V(t)^\dagger}{\mathrm{Tr}[V(t)^\dagger V(t)\rho(0)]}, \tag{4.13}$$

where

$$\begin{aligned} V(t) &= e^{-\gamma\sigma_+\sigma_- t}e^{R\sigma_-} \\ &= (e^{-\gamma t}\sigma_+\sigma_- + \sigma_-\sigma_+)(1 + R\sigma_-) \end{aligned} \tag{4.14}$$

and R is a random variable whose probability density at time t is

$$P(R,t) = \mathrm{Tr}[V(t)^\dagger V(t)\rho(0)]\frac{e^{-R^2/(2\kappa)}}{\sqrt{2\pi\kappa}}, \tag{4.15}$$

where we have defined $\kappa \equiv (1-e^{-2\gamma t})$. When the initial state is the single-qubit maximally mixed state, $\rho(0) = I/2$, the solution is

$$\rho(t) = \frac{[e^{-2\gamma t}\sigma_+\sigma_- + e^{-\gamma t}(\sigma_+ + \sigma_-) + (1+R^2)\sigma_-\sigma_+]}{2 + R^2 - \kappa} \tag{4.16}$$

and

$$P(R,t) = \frac{(2 + R^2 - \kappa)}{\sqrt{8\pi\kappa}}e^{-R^2/(2\kappa)}, \tag{4.17}$$

The evolution of the average value of the linear entropy is then given by

$$\langle L(t)\rangle = \int_{-\infty}^{\infty}(1 - \mathrm{Tr}[\rho(t)^2])P(R,t)dR. \tag{4.18}$$

This integral cannot be solved analytically, and we will therefore evaluate it numerically. We plot in Fig 4.3 the evolution of linear entropy as a function of time.

When η is less than unity the SME is no longer equivalent to an SSE because it can increase the entropy of an initially pure state. Nevertheless, it turns out that it is possible to obtain an analytic solution to the SME by using the above technique of solving a linear

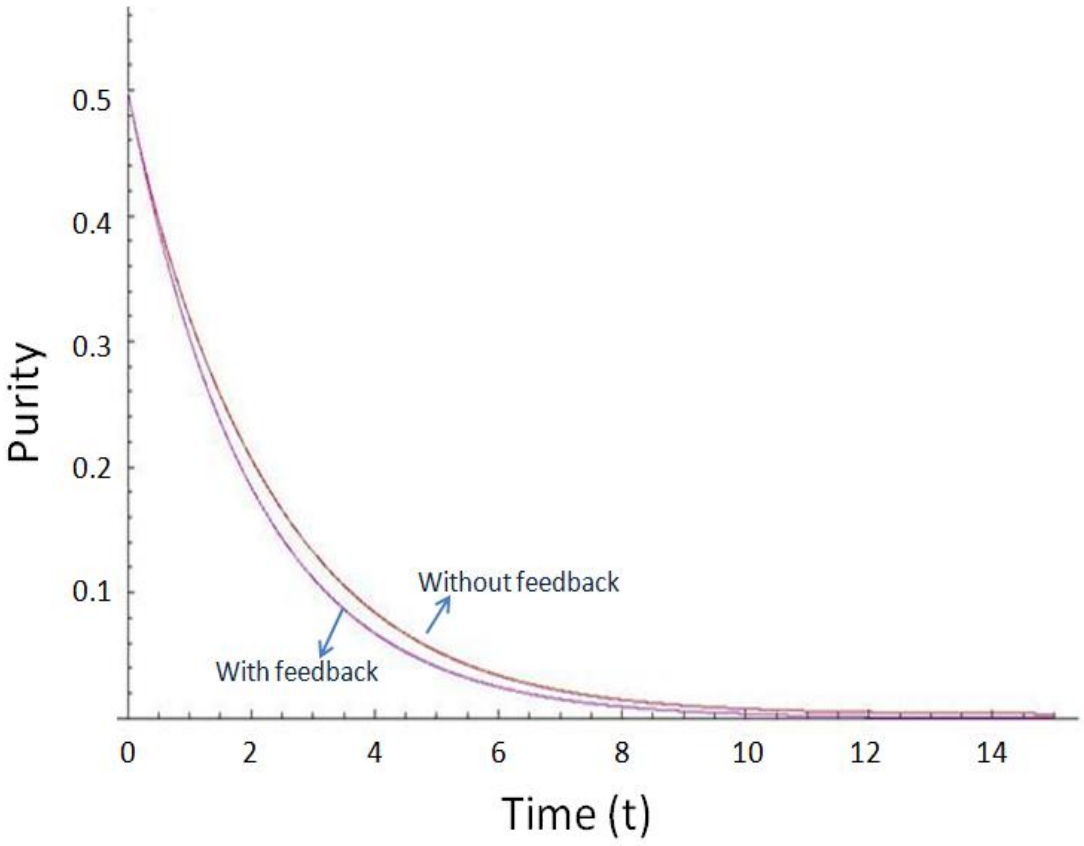

FIGURE 4.3. The plot showing the speedup from using the feedback. The mozanta curve is with feedback and the red curve is without feedback for a unit detector efficiency,$\eta = 1$. From this plot it is clear that feedback increases the rate of purification.

SSE. As far as we know this method has not appeared in the literature to date, and so we describe it in detail in the appendix.

When the initial state is $\rho(0) = I/2$ the solution for abitrary η is

$$\begin{aligned} \rho(t) &= (2\mathcal{N})^{-1} \left[e^{-2\gamma t}\sigma_+\sigma_- + e^{-\gamma t}\left(\sigma_+ + \sigma_-\right) \right. \\ &\qquad \left. + \left(1 + R^2 + [1-\eta]\kappa\right)\sigma_-\sigma_+ \right], \end{aligned} \tag{4.19}$$

where $\mathcal{N} = 1 + R^2/2 - \eta\kappa/2$ is the normalization constant. The probability density for the random variable R is now

$$P(R,t) = \frac{2 + R^2 - \eta\kappa}{\sqrt{8\pi\eta\kappa}} e^{-R^2/(2\eta\kappa)} \tag{4.20}$$

We define the speed-up afforded by the rapid purification as the ratio of two times, $s = t_{\rm m}/t_{\rm fb}$. The first time, $t_{\rm m}$, is that taken for $\langle L(t)\rangle$ to reach a given target value in the

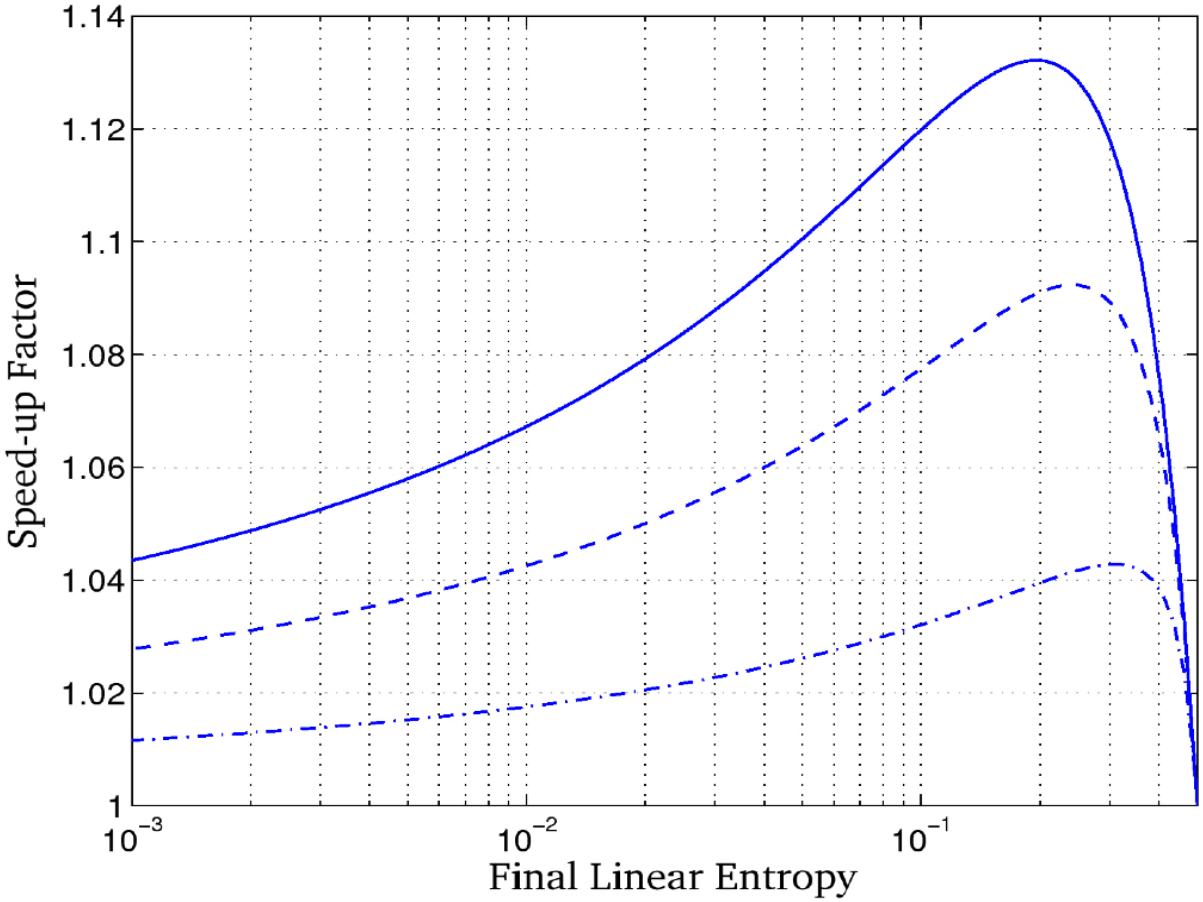

FIGURE 4.4. The speed-up factor in the time required to achieve a given final value of the average linear entropy, $\langle L \rangle$, afforded by the deterministic rapid-purification algorithm when the initial state of the optical qubit is completely mixed, as a function of $\langle L \rangle$. The various curves correspond to different values of the measurement efficiency η. Solid line: $\eta = 1$; Dashed line: $\eta = 0.8$; Dash-dot Line: $\eta = 0.5$.

absence of feedback, and the second time, $t_{\rm fb}$, is that taken for $L_{\rm fb}(t)$ to reach the same target value. Using the expressions for the linear entropy in the two cases (Eqs. (4.11) and (4.18)) we plot this speed-up as a function of the target entropy in Figure 4.4, and for three values of the detection efficiency η. We see that in the present case the speed-up factor reaches a peak and then decays back to unity as time increases. This is quite different behavior to that of the equivalent protocol for a measurement of an observable (a non-dissipative measurement), which tends to its maximum value as $t \to \infty$.

4.3 Solving the Stochastic Master Equation for Inefficient Detection

We first note that a master equation that describes inefficient detection is equivalent to a master equation containing two simultaneous measurements, where the observer has access to only one, and must average over the results of the other [92]. Our method is then to solve the Stochastic Schrödinger equation equivalent to the SME with two measurements (by using the method of linear quantum trajectories [106, 107, 108, 92]), and then take the average over the second measurement at the end to obtain the solution for inefficient detection. It turns out that the resulting integrals are straightforward and give a fully analytic solution. The SME Eq.(4.2) is thus equivalent to the linear SSE [92])

$$d|\psi\rangle = \left[-\gamma a^\dagger a dt + \sqrt{2\eta\gamma}\, a dW + \sqrt{2(1-\eta)\gamma}\, a dV\right]|\psi\rangle \tag{4.21}$$

where dW and dV are independent Gaussian noise sources so that $dW dV = 0$. The observer has access to the measurement record corresponding the measurement associated with dW, and thus must ultimately average over dV. We obtain the evolution operator which solves this equation by using the method given in reference [108], and this is

$$V(t,R,Q) = e^{-\gamma a^\dagger a t} e^{\kappa a^2} e^{aR} e^{aQ} \tag{4.22}$$

where

$$R = \sqrt{2\eta\gamma}\int_0^t e^{-2\gamma s} dW(s) \tag{4.23}$$

$$Q = \sqrt{2(1-\eta)\gamma}\int_0^t e^{-2\gamma s} dV(s) \tag{4.24}$$

and $\kappa \equiv (1 - e^{-2\gamma t})$. The probability densities for R and Q resulting from the above stochastic integrals are Gaussian, with mean zero and variances $V_R = \eta\kappa$ and $V_Q = (1-\eta)\kappa$. We will denote these Gaussian densities by $G(R)$ and $H(Q)$, respectively.

For an initial state $\rho(0)$, the solution is thus

$$\rho(t,R,Q) = \frac{V\rho(0)V^\dagger}{\mathcal{N}} \tag{4.25}$$

where $\mathcal{N} = \mathrm{Tr}[V^\dagger V \rho(0)]$ is the normalization. The true joint probability density for R and Q is given by the product of the Gaussian densities $G(R)$ and $H(Q)$, multiplied by $\mathcal{N}$. That is

$$P(R,Q,t) = \mathrm{Tr}[V^\dagger V \rho(0)] G(R) H(Q). \tag{4.26}$$

To obtain the solution to the inefficient SME we must average over the Q keeping R fixed. This solution is therefore

$$\begin{aligned} \sigma(R,t) &= \int_{-\infty}^{\infty} \rho(R,Q,t) P(Q|R) dQ \\ &= \frac{1}{P(R)} \int_{-\infty}^{\infty} \rho(R,Q,t) P(R,Q) dQ \\ &= \frac{G(R)}{P(R)} \int_{-\infty}^{\infty} V\rho(0)V^\dagger H(Q) dQ \\ &= \frac{1}{\mathcal{M}} \int_{-\infty}^{\infty} V\rho(0)V^\dagger H(Q) dQ \end{aligned} \tag{4.27}$$

where $\mathcal{M}$ is merely the normalization. From this we see that we need only perform an integration over the Gaussian density for Q, which is straightforward.

4.4 Conclusion

We have considered applying feedback to the homodyne detection of a single optical qubit so as to change the rate at which the system is purified (so called "rapid-purification feedback algorithms"). We have shown that there exists a feedback algorithm that increases the rate at which the *average purity* increases, and like its non-dissipative counterpart this results in a deterministic evolution for the purity of the system. Unlike its non-disspative analogue, the speed-up provided by this protocol reaches its maximum value at a finite time, decaying to unity as $t \to \infty$. We also found that the speed-up remains for measurement efficiencies well below unity, although the speed-up decreases as the efficiency drops. We found that this protocol behaves much more like those for a non-dissipative measurement, in that the speed-up factor increases monotonically and tends to a value of two in the long-time limit. This protocol is, however, more sensitive to noise than

the previous protocols. The above results show that it should be feasible to demonstrate rapid-purification protocols in an optical setting.

References

[1] P. A. M. Dirac, Proceedings of Royal Society(London) A **114**, 243 (1927).

[2] R. J. Gluber, Phys.Rev **130**, 2529 (1963).

[3] C. M. Caves, Phys. Rev. D **23**, 1693 (1981).

[4] H. Lee, P. Kok, and J. P.Dowling, J.Mod.Opt. **49**, 2325 (2002).

[5] E. by Stephen M. Barnett and J. A. Vaccaro, *The Quantum Phase Operator* (Taylor & Francis).

[6] P. A. M. Dirac, *The Principles of Quantum Mechnics* (Oxford University Press, Oxford, UK).

[7] R. P. Feynman, Int. J Theoretical Physics **21**, 467 (1982).

[8] R. P. Feynman, Opt. News **11**, 11 (1985).

[9] P. W. Shor, Proc. 35th Annual Symposium on Founadations of Computer Science (Shafi Goldwasser) (1994).

[10] M. A.Nielsen and I. L. Chaung, *Quantum Computation and Quantum Information*, First ed. (Cambridge University press, Cambridge UK, 2000).

[11] S. Lloyd, Science **273**, 1073 (1996).

[12] K. Jacobs and D. A. Steck, Contemporary Physics **47** (2006).

[13] C. M. Caves and G. J. Milburn, Phys. Rev. A **36**, 5543 (1987).

[14] C. W. Gardiner and P. Zoller, *Quantum Noise* (Springer-Verlag, Heidelberg).

[15] S. Haroche and J.-M. Raimond, *Exploring the Quantum* (Oxford university press).

[16] W. H. Louisell, Phys. Lett. **7** (1963).

[17] L. Susskind and J. Glogower, Physics **1** (1964).

[18] P. Carruthers and M. M. Nieto, Phys. rev. Lett. **14**, 387 (1965).

[19] S. M. Barnett and D. T. Pegg, J. Phys. A: Math. Gen. **19**, 3849 (1986).

[20] D. T. Pegg and S. M. Barnett, Europhys. Lett. **6**, 483 (1988).

[21] S. M. Barnett and D. T. Pegg, J. Mod. Opt. **36** (1989).

[22] D. T. Pegg and S. M. Barnett, Phys. Rev. A **39**, 1665 (1989).

[23] J. A. Vaccaro and D. T. Pegg, J. Mod. Opt. **37** (1990).

[24] H. M. W. D. W. Berry and Z.-X. Zhang, Phys. Rev. A **60**, 2458 (1999).

[25] Z. Y. O. C. K. Hong and L. Mandel, Phys. Rev. Lett. **59**, 2044 (1987).

[26] B. Yurke, S. L. McCall, and J. R. Klauder, Phys. Rev. A **33**, 4033 (1986).

[27] H. P. Yuen, Phys. Rev. Lett. **56**, 2176 (1986).

[28] J. P. Dowling, Phys. Rev. A **57**, 4736 (1998).

[29] B. C. Sanders, Phys. Rev. A **40**, 2417 (1989).

[30] D. W. Berry and H. M. Wiseman, Phys. Rev. Lett. **85**, 5098 (2000).

[31] D. W. Berry, H. M. Wiseman, and J. K. Breslin, Phys. Rev. A **63**, 053804 (2001).

[32] M. A. Rubin and S. Kaushik, Phys. Rev. A **75**, 053805 (2007).

[33] M. H. G. Gilbert and Y. Weinstein, JOSA B **25**, 1336 (2008).

[34] S. D. Huver, C. F. Wildfeuer, and J. P. Dowling, Phys. Rev. A **78**, 063828 (2008).

[35] V. Giovannetti, S. Lloyd, and L. Maccone, Phys. Rev. Lett **96**, 010401 (2006).

[36] M. J. Holland and K. Burnett, Phys. Rev. Lett. **71**, 1355 (1993).

[37] J. J. . Bollinger, W. M. Itano, D. J. Wineland, and D. J. Heinzen, Phys. Rev. A **54**, R4649 (1996).

[38] P. Bouyer and M. A. Kasevich, Phys. Rev. A **56**, R1083 (1997).

[39] C. C. Gerry, Phys. Rev. A **61**, 043811 (2000).

[40] J. A. Dunningham, K. Burnett, and S. M. Barnett, Phys. Rev. Lett. **89**, 150401 (2002).

[41] D. Leibfried *et al.*, Science **304**, 1476 (2004).

[42] R. C. Pooser and O. Pfister, Phys. Rev. A **69**, 043616 (2004).

[43] R. P. A. G. G. J. P. J. L. O. a. A. G. W. K. J. Resch, K. L. Pregnell, Phys. Rev. Lett **98**.

[44] H. Uys and P. Meystre, Phys. Rev. A **76**.

[45] G. A. Durkin and J. P. Dowling., Phys. Rev. Lett. **99**, 070801 (2007).

[46] J. L. O'Brien, Science **318**, 1393 (2007).

[47] U. Dorner *et al.*, Optimal Quantum Phase Estimation (unpublished); quant-ph/0807.3659 (2008).

[48] A. S. Lane, S. L. Braunstein, and C. M. Caves, Phys. Rev. A **47**, 1667 (1993).

[49] B. C. Sanders and G. J. Milburn, Phys. Rev. Lett. **75**, 2944 (1995).

[50] Z. Hradil, Phys. Rev. A **51**, 1870 (1995).

[51] T. Kim, O. Pfister, M. J. Holland, J. Noh, and J. L. Hall, Phys. Rev. A **57**, 4004.

[52] L. Pezze and A. Smerzi, Phys. Rev. A **73**, 011801(R) (2006).

[53] T. Nagata, R. Okamoto, J. L. O'Brien, K. Sasaki, and S. Takeuchi, Science **316**, 726 (2007).

[54] F. W. Sun *et al.*, Euro. Phys. Lett. **82**, 24001 (5pp) (2008).

[55] H. J. Kimble, Y. Levin, A. B. Matsko, K. S. Thorne, and S. P. Vyatchanin, Phys. Rev. D **65**, 022002 (2001).

[56] A. N. Boto *et al.*, Phys. Rev. Lett. **85**, 2733 (2000).

[57] C. C. Gerry and R. A. Campos, Phys. Rev. A **64**, 063814.

[58] P. Kok, H. Lee, and J. P. Dowling, Phys. Rev. A **65**, 052104 (2002).

[59] J. Fiurášek, Phys. Rev. A **65**, 053818 (2002).

[60] M. A. R. U. S. G. A. Z. Philip Walther, Jian-Wei Pan, Nature **429**, 158 (2004).

[61] J. S. L. M. W. Mitchell and A. M. Steinberg, Nature **429**, 161 (2004).

[62] F. W. Sun, Z. Y. Ou, and G. C. Guo, Phys. Rev. A **73**, 023808 (2006).

[63] *et al.*. D. Leibfried, Nature **438**, 639 (2005).

[64] G. Gilbert, M. Hamrick, and Y. S. Weinstein, J. Opt. Soc. Am. B **25**, 1336 (2008).

[65] C.C.Gerry and P.L.Knight, *Introductory Quantum Optics*, First ed. (Cambridge University press, Cambridge UK, 2005).

[66] B.L.Higgins, D.W.Berry, S.D.Barlett, H.M.Wiseman, and G.J.Pryde, Nature **450**, 393 (2007).

[67] The rotation matrix element:
$\langle j\nu|e^{-i\theta\hat{J}_y}|j\mu\rangle = d^j_{\nu\mu}(\theta) = (-1)^{\nu-\mu}2^{-\nu}\sqrt{\frac{(j-\nu)!(j+\nu)!}{j-\mu)!(j+\mu)!}} \times P^{(\nu-\mu,\nu+\mu)}_{j-\nu}(cos\theta)(1 - cos\theta)^{\frac{\nu-\mu}{2}}(1 + cos\theta)^{\frac{\nu+\mu}{2}}$ where $P^{(\alpha,\beta)}_n(x)$ is the Jacobi polynomial. These rotation matrix elements further possess symmetric relations:
$d^{j*}_{\nu\mu} = d^j_{\nu\mu} = (-1)^{\nu-\mu}d^j_{\nu\mu} = d^j_{\mu\nu}$; and a contraction rule: $\sum^j_{\nu=-j} d^j_{\alpha\nu}(\theta_1)d^j_{\nu\mu}(\theta_2) = d^j_{\alpha\mu}(\theta_1+\theta_2)$.

[68] D.M.Brink and G.R.Satchler, *Angular Momentum* (Clarendon Press, Oxford, UK, 1993).

[69] Y. Gao and H. Lee, J. Mod. Opt. **55**, 3319 (2008).

[70] R. A. Campos, C. C. Gerry, and A. Benmoussa, Phys. Rev. A **68**, 023810 (2003).

[71] G. M. D'Ariano, P. Lo Presti, and M. G. A. Paris, Phys. Rev. Lett. **87**, 270404 (2001).

[72] L. G. Lutterbach and L. Davidovich, Phys. Rev. Lett. **78**, 2547 (1997).

[73] D. A. *et al.*, J. Mod. Opt. **51**, 1499.

[74] H. L. *et al.*, J. Mod. Opt. **51**, 1517.

[75] M. W. *et al.*, J. Mod. Opt. **51**, 1549.

[76] D. Rosenberg, A. E. Lita, A. J. Miller, and S. W. Nam, Phys. Rev. A **71**, 061803 (2005).

[77] H. A. Bachor and T. C. Ralph, *A Guide to Experiments in Quantum Optics* (Wiley-VCH, 2004).

[78] P. K. *et al.*, Rev. Mod. Phys. **79**.

[79] A. Royer, Phys. Rev. A **15**, 449 (1977).

[80] Chapter 6 in *Quantum State Estimation*, Springer Verlag, Series: Lecture Notes in Physics , Vol. 649, Edited by: Paris, Matteo; Rehacek, Jaroslav.

[81] Z. Hradil, Phys. Rev. A **51**, 1870 (1995).

[82] Z. *et al.*. Hradil, Phys. Rev. Lett. **76**, 4295 (1996).

[83] S. L. Vittorio Giovannetti and L. Maccone, Science **306**.

[84] C. W. Helstrom, *Quantum Detection and Estimation Theory*, First ed. (Acedemic,, New York, USA, 1976).

[85] J. H. Shapiro, Phys. Scr. **T48**, 105 (1993).

[86] B. C. Sanders and G. J. Milburn, Phys. Rev. Lett. **75**, 2944 (1995).

[87] G. J. M. B. C. Sanders and Z. Zhang, **44**, 1309 (1997).

[88] A. S. Holevo, Lecture Notes Math. **1055** (1984).

[89] R. Loudon, , 3rd ed. (Oxford University Press, oxford, UK, 2000).

[90] K. L. Pregnell and D. T. Pegg, Phys. Rev. Lett. **89**, 173601 (2002).

[91] S. Lloyd, Phys. Rev. A **62**, 022108 (2000).

[92] K. Jacobs and D. Steck, Contemporary Physics **47**, 279.

[93] H. M. Wiseman and G. J. Milburn, Phys. Rev. Lett. **70**, 548 (1993).

[94] K. Jacobs, Phys. Rev. A **67**, 030301 (2003).

[95] J. Combes and K. Jacobs, Phys. Rev. Lett. **96**, 010504 (2006).

[96] H. M. Wiseman and J. F. Ralph, New. J. Phys **8**, 90 (2006).

[97] A. N. Jordan and A. N. Korotkov, Phys. Rev. B **74**, 085307 (2006).

[98] J. F. Ralph E. J. Griffith, C. D. Hill, and T. D. Clark, in *Proceedings of SPIE: Quantum Information and Computation IV* , edited by E. J. Donkor, A. R. Pirich and H. E. Brandt (SPIE 2006), vol. 6244, p. 624403.

[99] C. Hill and J. F. Ralph, New. J. Phys **9**, 151 (2007).

[100] E. J. Griffith, C. D. Hill, J. F. Ralph, H. M. Wiseman, and K. Jacobs, Phys. Rev. B **75**, 014511 (2007).

[101] C. D. Hill and J. F. Ralph, (in preparation) (2007).

[102] H. M. Wiseman and L. Bouten, arxiv: 0707.3001(2007).

[103] T. A. Brun, Am. J. Phys. **70**, 719 (2002).

[104] V. P. Belavkin, in *Information, Complexity and Control in Quantum Physics*, edited by A. Blaquiere, S. Diner, and G. Lochak (Springer-verlag, New York, 1987).

[105] H. M. Wiseman and G. J. Milburn, Phys. Rev. A **47**, 642 (1993).

[106] H. M. Wiseman, Quantum Semiclass. Opt. **8**, 205 (1996).

[107] P. Goetsch and R. Graham, Phys. Rev. A **50**, 5242 (1994).

[108] K. Jacobs and P. L. Knight, Phys. Rev. A **57**, 2301 (1998).

Appendix: Permission to use the Published Work

The following is the FAQ section of the American Physical Society (APS), which can be found at http://publish.aps.org/copyrightFAQ.html . Here I am copying only the relevant question and the response, which allows me to use my work published in Physical Review A **77**, 012102(2008)

Q: As the author of an APS-published article, may I include my article or a portion of my article in my thesis or dissertation?

A: Yes, the author has the right to use the article or a portion of the article in a thesis or dissertation without requesting permission from APS, provided the bibliographic citation and the APS copyright credit line are given on the appropriate pages.

Vita

Aravind Chiruvelli is a native of Kotra village of Andhra Pradesh state in India. He was born in June 1978. He finished his undergraduate studies in mathematics, physics, and geology at Osmania University in May 2000. He earned a master of science degree in physics from University of Hyderabad in may 2002. He further earned Master of Science in Applied Physics, degree from University of Massachusetts, Boston, in December 2005. In January 2006 he came to Louisiana State University to pursue graduate studies in physics. He is currently a candidate for the degree of Doctor of Philosophy in physics, which will be awarded in December 2009.